

See discussions, stats, and author profiles for this publication at: <https://www.researchgate.net/publication/231665239>

# Raman Spectroscopic Measurements of Scandium(III) Hydration in Aqueous Perchlorate Solution and ab Initio Molecular Orbital Studies of Scandium(III) Water Clusters: Does Sc(III) Oc...

ARTICLE in THE JOURNAL OF PHYSICAL CHEMISTRY A · SEPTEMBER 1999

Impact Factor: 2.69 · DOI: 10.1021/jp9916541

---

CITATIONS

35

---

READS

55

## 2 AUTHORS:



**Wolfram Rudolph**

Technische Universität Dresden

127 PUBLICATIONS 1,323 CITATIONS

SEE PROFILE



**Cory Christopher Pye**

Saint Mary's University

79 PUBLICATIONS 1,947 CITATIONS

SEE PROFILE

# Raman Spectroscopic Measurements of Scandium(III) Hydration in Aqueous Perchlorate Solution and ab Initio Molecular Orbital Studies of Scandium(III) Water Clusters: Does Sc(III) Occur as a Hexaaqua Complex?

Wolfram W. Rudolph<sup>\*,†</sup> and Cory C. Pye<sup>‡</sup>

TU Dresden, Universitätsklinikum Carl Gustav Carus, Institut für Virologie, Gerichtsstr. 5, D-01069 Dresden, Germany, and St. Mary's University, Department of Chemistry, 923 Robie Street, Halifax, Nova Scotia, B3H 3C3, Canada

Received: May 13, 1999; In Final Form: September 21, 1999

We have shown that Sc(III) in aqueous perchlorate solution occurs as a hexaaqua cation. The weak, polarized Raman band assigned to the  $\nu_1(a_{1g})(\text{ScO}_6)$  mode of the hexaaqua Sc(III) ion has been studied as a function of concentration. Besides the isotropic component at 442  $\text{cm}^{-1}$ , two weak depolarized modes at 295 and 410  $\text{cm}^{-1}$  were measured in the Raman effect. These two modes of the  $\text{ScO}_6$  unit were assigned to  $\nu_5(f_{2g})$  and  $\nu_2(e_g)$ , respectively. The infrared active mode,  $\nu_3(f_{1u})$ , was found at 460  $\text{cm}^{-1}$ . The Raman spectroscopic data suggest that the hexaaqua Sc(III) ion is stable in perchlorate solution within the concentration range measured. Furthermore, the frequency data confirm the centrosymmetry of the Sc(III) aqua complex, contrary to earlier Raman results. The  $\text{ScO}_6$  unit possesses  $O_h$  symmetry (water seen as point mass). These findings are in contrast to  $\text{ScCl}_3$  solutions, where chloride replaces water in the first hydration sphere and forms one or more chloro complexes. Gas-phase structures, binding energies, and enthalpies are reported for small  $[\text{Sc}(\text{OH}_2)_n]^{3+}$  clusters, with one to nine water molecules in the first sphere. Ab initio molecular orbital calculations were performed at the HF and MP2 levels of theory using different basis sets up to 6-31+G\*. The water molecules in these clusters coordinate the  $\text{Sc}^{3+}$  in highly symmetric arrangements that tend to enhance electrostatic charge–dipole interactions while minimizing ligand–ligand repulsion. The Sc–O bond length for the  $[\text{Sc}(\text{OH}_2)_6]^{3+}$  cluster reproduces the experimentally determined bond length (EXAFS) of 2.18 Å. The theoretical binding energy for the  $[\text{Sc}(\text{OH}_2)_6]^{3+}$  ion was calculated and accounts for ca. 54–59% of the experimental single ion hydration enthalpy of Sc(III). The stability of the hexaaquascandium(III) cluster could be demonstrated by comparing the stability of the  $[\text{Sc}(\text{OH}_2)_6(\text{OH}_2)]^{3+}$  cluster with the  $[\text{Sc}(\text{OH}_2)_7]^{3+}$  cluster, resulting in the stability of the former. The frequencies of  $\nu_1(\text{ScO}_6)$  of the  $[\text{Sc}(\text{OH}_2)_6]^{3+}$  cluster are ca. 11% lower than the experimental frequency. The reason for this discrepancy was discussed and found to lie in the lack of the second hydration sphere which was subsequently modeled as the  $[\text{Sc}(\text{OH}_2)_{18}]^{3+}$  cluster, denoted Sc[6+12]. Frequencies of the  $\text{ScO}_6$  unit for the Sc[6+12] cluster were calculated and agree with the experimental values. The binding enthalpy resembles that of the single ion hydration enthalpy.

## 1. Introduction

In the last 2 decades, many experimental studies using X-ray and neutron scattering have been carried out to describe the hydration structure of nearly all stable metal ions. Despite great research effort and its fundamental importance, the first hydration number of Sc(III) in aqueous solution is still a subject of controversy (cf. data in refs 1 and 2). Raman spectroscopic results<sup>3</sup> and a recent X-ray absorption fine structure measurement<sup>4</sup> proposed a probable first hydration number of 7. It is known that Sc(III) is quite similar to Al(III) because of its small ionic radius ( $\sim 0.73$  Å).<sup>5</sup> In the solid state, oxygen-coordinated Sc(III) compounds occur in coordination numbers equal to 3, 6, 7, 8, and 9, with the six coordination being the most common (octahedral or trigonal prism), while the next common type is the eight coordination (cubic, square antiprism and dodecahedral coordination polyhedron).<sup>6</sup> The average Sc(III)–O bond length is 2.11 Å for the six coordination and 2.24 Å for the eight

coordination. The results of a recent crystal structure of scandium(III) trifluoromethanesulfonate enneahydrate,  $\text{Sc}(\text{OH}_2)_9(\text{CF}_3\text{SO}_3)_3$ ,<sup>7</sup> reveal that  $\text{Sc}^{3+}$  is surrounded by nine water molecules (tricapped trigonal prism) with six short Sc<sup>3+</sup>–O bonds (2.171 Å) and three longer bonds (2.47 Å). <sup>1</sup>H NMR measurements<sup>8</sup> on Sc(III) perchlorate and nitrate in water/acetone mixtures were carried out, but the coordination number of the first hydration sphere could not be determined because of the rapid proton exchange between bulk and water in the first coordination sphere, even at  $-100$  °C for perchlorate solutions. In nitrate solutions, unusually low hydration values of 3.9–5.1 were detected, which clearly indicated that hydrolysis and nitrate complex formation were important in this solution. Kanno and co-workers<sup>3a</sup> measured the Raman spectra of aqueous  $\text{Sc}^{3+}$  and  $\text{Al}^{3+}$  chloride solutions in vitreous state in order to avoid the interference of the strong quasielastic Rayleigh wing, which extends well over 500  $\text{cm}^{-1}$ .

Raman spectroscopy has been extensively used to elucidate the spectroscopic characteristics of cations in aqueous solutions. However, in solution, the strong quasielastic Rayleigh wing prohibits the clear detection of the weak low-frequency modes

\* Corresponding author. E-mail: Wolfram.Rudolph@mailbox.tu-dresden.de.

<sup>†</sup> Universitätsklinikum Carl Gustav Carus.

<sup>‡</sup> St. Mary's University.

of the metal aqua ions.<sup>9</sup> To circumvent this difficulty, Raman difference spectroscopy has been developed.<sup>10,11</sup> The subtraction of a synthetic background has also been employed to obtain baseline corrected Raman spectra.<sup>12–14</sup>

It is known that dissolved ions (especially anions) alter the low-frequency Raman spectrum of water.<sup>15</sup> Therefore, the Raman difference spectra obtained by subtracting the spectrum of pure water from the spectrum of an aqueous solution must be viewed with caution as pointed out in previous papers.<sup>9,16</sup> On the other hand, it is not necessary to employ Raman difference spectroscopy or to subtract a synthetic Rayleigh wing from the aqueous electrolyte spectra in order to obtain baseline corrected spectra. It has been shown<sup>17</sup> that for accurate relative intensity measurements it is essential to normalize the low-frequency Raman data ( $R$  spectra) for the Bose–Einstein temperature factor,  $B$ , and a frequency factor in order to present the data in a spectral form that is directly related to the relative molar scattering factor,  $S_Q(\bar{\nu}) \propto (\partial\alpha/\partial Q_i)^2$ , where  $Q_i$  is the mass-weighted normal coordinate.

In this study, Raman spectra of scandium perchlorate and chloride solutions were obtained as a function of concentration in order to draw conclusions about the stability of its aqua complex. It is known that perchlorate does not penetrate the first hydration sphere, which allows a vibrational characterization of the aqua scandium species. In scandium chloride solutions, the situation is not so clear, because of possible chloro complex formation,<sup>18</sup> though Kanno et al.<sup>3</sup> stated that chloride does not penetrate the first hydration sphere of scandium(III).

Additionally, we modeled the vibrational spectra of aqua Sc(III) ions using ab initio molecular orbital calculations. Ab initio calculations, whose utility for predicting structural and vibrational characteristics are already well-established,<sup>9,19,20</sup> were performed on Sc(III) water clusters in order to support our spectroscopic data. For this purpose, Hartree–Fock and second-order Møller–Plesset levels of theory were employed with several different basis sets. The aim of our spectroscopic studies and ab initio molecular orbital calculations is to establish the coordination number of the first hydration sphere of Sc(III) in aqueous perchlorate solutions.

## 2. Experimental Section, Data Treatment, and ab Initio Calculations.

The  $\text{Sc}(\text{ClO}_4)_3$  stock solution was prepared by dissolving  $\text{Sc}_2\text{O}_3$  with a stoichiometric amount of  $\text{HClO}_4$ . The solution contains an excess of ca. 10%  $\text{HClO}_4$  in order to prevent hydrolysis of Sc(III). The density of the solution was determined with a standardized 5 mL pycnometer at 20 °C. The Sc(III) content of the solution was determined by colorimetric titration with standard EDTA and xylenol orange as an indicator.<sup>21</sup> The solution's pH was measured with a glass electrode and was ca. 0.8. The perchlorate concentration was determined by passing a portion of the solution through a column with a strong cation exchanger (Dowex 50W-X8) and titrating the eluate with standardized NaOH solution. The  $\text{Sc}(\text{ClO}_4)_3$  stock solution was 1.65 mol/L (1.905 mol/kg) with an excess of 10%  $\text{HClO}_4$ . A deuterated solution was prepared by dissolving the  $\text{Sc}(\text{ClO}_4)_3$  in  $\text{D}_2\text{O}$  (Cambridge Isotope Laboratories, 99.9%) and evaporating the water off in a vacuum distillation apparatus. This process was repeated three times. The deuteration grade, checked by Raman spectroscopy (in the OD and OH region), was better than 99.0%.

The  $\text{ScCl}_3$  stock solution was prepared by dissolving  $\text{Sc}_2\text{O}_3$  with an excess amount of HCl. The solution was analyzed for scandium by colorimetric titration with standard EDTA.<sup>21</sup> The

chloride content was determined with a standardized  $\text{AgNO}_3$  solution after the method by Fajans.<sup>22</sup> The solution densities were determined with a pycnometer (5 mL) at 20 °C. The stock solution was 2.550 mol/L (2.801 mol/kg) and contained an excess of 10% HCl to prevent hydrolysis. With the  $\text{ScCl}_3$  stock solution and a LiCl stock solution, we prepared a  $\text{ScCl}_3$  solution with excess chloride (as LiCl) by weight. The mole ratio in the solution was found to be  $\text{ScCl}_3/\text{LiCl}/\text{H}_2\text{O} = 0.01428:0.10594:0.8798$ , for example, a mole ratio of  $\text{Sc(III)}/\text{Cl(I)} = 1:10.4$ .

Great care was taken to characterize the solutions in order to account for possible processes occurring in the solutions, such as complexation, hydrolysis, and precipitation of basic salt.<sup>23,24</sup>

All solutions were filtered through a 0.22  $\mu\text{m}$  Millipore filter into a 150 mm ID quartz tube before Raman spectroscopic measurement.

Raman spectra were obtained with a Coderg PHO Raman spectrometer using the 488.0 and 514.5 nm argon ion laser line with a power level at the sample about 0.9 W. The mechanical slit of the double monochromator was normally set to give a spectral slit width of 1.8  $\text{cm}^{-1}$ . The scattered light was detected with a PMT cooled to  $-20$  °C, integrated with a photon counter and processed with a boxcar averager interfaced to a personal computer. Two data points were collected per wavenumber. To increase the signal-to-noise ratio, six data sets were collected for each scattering geometry ( $I_{||}$  and  $I_{\perp}$ ). A quarter wave plate before the slit served to compensate for grating preference.  $I_{||}$  and  $I_{\perp}$  spectra were obtained with fixed polarization of the laser beam by changing the polaroid film at 90° between the sample and the entrance slit to give the scattering geometries

$$I_{||} = I(Y[ZZ]X) = 45\alpha'^2 + 4\beta'^2 \quad (1)$$

$$I_{\perp} = I(Y[ZY]X) = 3\beta'^2 \quad (2)$$

The isotropic spectrum  $I_{\alpha}$  was constructed as follows:

$$I_{\alpha} = I_{||} - \frac{4}{3}I_{\perp} \quad (3)$$

The reduced or  $R_Q(\bar{\nu})$  spectrum was constructed after eq 4,

$$R_Q(\bar{\nu}) = I(\bar{\nu})(\bar{\nu}_o - \bar{\nu}_i)^{-4}\bar{\nu}_i B \quad (4)$$

Equation 1 is valid under the condition that the normal coordinates are taken to be harmonic and the polarizability expansion is terminated after the first-order term (i.e., the double harmonic approximation). The  $R_Q(\bar{\nu})$  spectrum has been related to the vibrational density of states spectrum and may also be considered as the energy absorbed in a scattering process (see ref 17 and references therein). The corresponding spectra in  $R$  format are constructed in a similar fashion according to eqs 1–3. Further spectroscopic details about the high-temperature measurement, the band fit procedure, and details about  $R$  normalized Raman spectra are described in previous publications.<sup>16</sup>

For quantitative measurements, the perchlorate band,  $\nu_1(\text{ClO}_4^-)$  at 935  $\text{cm}^{-1}$  was used as an internal standard. From the  $R_{\text{iso}}$  spectra, the relative isotropic scattering coefficient  $S(\nu_1(\text{ScO}_6))$  was obtained. The use of  $S$  values instead of  $J$  values has the advantage that these relative scattering coefficients can be put on an absolute scale if an absolute standard reference is considered. For further details about  $S$  values cf.<sup>16a</sup>

Ab initio Hartree–Fock calculations with the STO-3G,<sup>25</sup> 3-21G,<sup>26</sup> and 6-31G\*<sup>27</sup> basis sets were employed. Huzinaga's (533321/5211\*/41) basis set was used for scandium<sup>28</sup> in conjunction with the 6-31G\* water basis set. All geometries were optimized with the GAUSSIAN 92 program,<sup>29</sup> and the

nature of the stationary points was confirmed by analytic frequency calculation where possible. A diffuse sp shell was added to the oxygen to give the standard HF/6-31+G\* basis set (no diffuse functions were added to scandium because its cationic nature renders them unnecessary). Finally, Møller–Plesset perturbation theory was used to approximate correlation effects (as MP2/6-31G\* and MP2/6-31+G\*). The frozen core approximation was used throughout. The shorthand notation L/B will be used to denote a calculation L/B//L/B, where an energy calculation is done at L/B, the same level as the geometry optimization.

For a given stoichiometry, there may be several corresponding local minima. This is known as the multiple minimum problem and is difficult to avoid. Our approach is to optimize structures in the highest reasonable symmetry unless better choices are previously available. Our initial choices were  $C_{2v}$ ,  $D_{2d}$ ,  $D_3$ ,  $S_4$ ,  $C_{2v}$ ,  $T_h$ ,  $C_{2v}$ ,  $D_{4h}$  and  $D_{2d}$ , and  $D_{3h}$  for the  $[\text{Sc}(\text{OH}_2)_n]^{3+}$  (with  $n = 1-9$ ).

For  $n = 2$ , two lower energy structures were found which were isoenergetic and possessed symmetry  $C_s$  and  $C_2$ . For  $n = 3$ , the MP2 calculations indicated that a slight out of plane desymmetrization to  $C_3$  was preferred.

For  $n = 7$ , the  $C_{2v}$  structure gave imaginary frequencies which were rectified by desymmetrization to  $C_2$ . For the octa and ennea structures, a total of four and eight structures were initially tried, corresponding to rotation about various water–Sc axes and to eclipsed and staggered Sc–O bonds. To minimize the computational cost, a “stepping stone” approach was utilized, whereby the STO-3G, 3-21G, and 6-31G\* geometry optimizations within the chosen symmetry were carried out, each using the analytic force constant matrix calculated from the previous level. The preferred structures had staggered bonds and exhibited an imaginary frequency corresponding to water twisting. Desymmetrization of these gave structures of symmetry  $S_8$  and  $D_3$ , respectively. All structures thus obtained were energy minima except the  $n = 9$  case. This  $D_3$  structure could not be desymmetrized further without eliminating water from the first sphere. The final symmetries found were thus  $C_{2v}$ ,  $C_s$ ,  $D_3$  (or  $C_3$ ),  $S_4$ ,  $C_{2v}$ ,  $T_h$ ,  $C_2$ ,  $S_8$ , and  $D_3$ .

The NBO (natural bond orbital) analysis of the water clusters is also given. The NBO method,<sup>30</sup> as implemented in Gaussian 92, was used to determine the atomic charges.

### 3. Results and Discussion

**3.1. Raman Spectroscopic Results.** *3.1.1.  $\text{Sc}(\text{ClO}_4)_3$  Solution.* Raman spectra of a 1.65 M  $\text{Sc}(\text{ClO}_4)_3$  solution were analyzed between 60 and 1300  $\text{cm}^{-1}$ . The “free”  $\text{ClO}_4^-$  ion possesses  $T_d$  symmetry and has nine modes of internal vibrations spanning the representation  $\Gamma_{\text{vib}}(T_d) = a_1 + e + 2f_2$ . All modes of vibration are Raman active, but in IR only the  $f_2$  modes are active. The spectrum of a 1.65 M  $\text{Sc}(\text{ClO}_4)_3$  solution shows the predicted four Raman-active bands for the tetrahedral  $\text{ClO}_4^-$ . A polarized overview Raman spectrum in R format at 25 °C is given in Figure 1a. In Figure 1b, the expanded wavenumber region from 60 to 700  $\text{cm}^{-1}$  for the two scattering geometries and the pure isotropic spectrum is given. The  $\nu_1(\text{ClO}_4^-)$  band centered at 935  $\text{cm}^{-1}$  is totally polarized, whereas  $\nu_3(f_2)(\text{ClO}_4^-)$  centered at 1114  $\text{cm}^{-1}$  is depolarized as are the deformation modes  $\nu_4(f_2)(\text{ClO}_4^-)$  at 630  $\text{cm}^{-1}$  and  $\nu_2(e)(\text{ClO}_4^-)$  at 463  $\text{cm}^{-1}$  [cf. ref 31 and references therein].

In the isotropic Raman scattering, a mode at  $442 \pm 2 \text{ cm}^{-1}$  (fwhh =  $74 \pm 2 \text{ cm}^{-1}$ ) becomes visible (Figure 1). In the depolarized scattering geometry, two modes are to be observed, a weak broad mode at  $295 \pm 5 \text{ cm}^{-1}$  and a very weak mode at

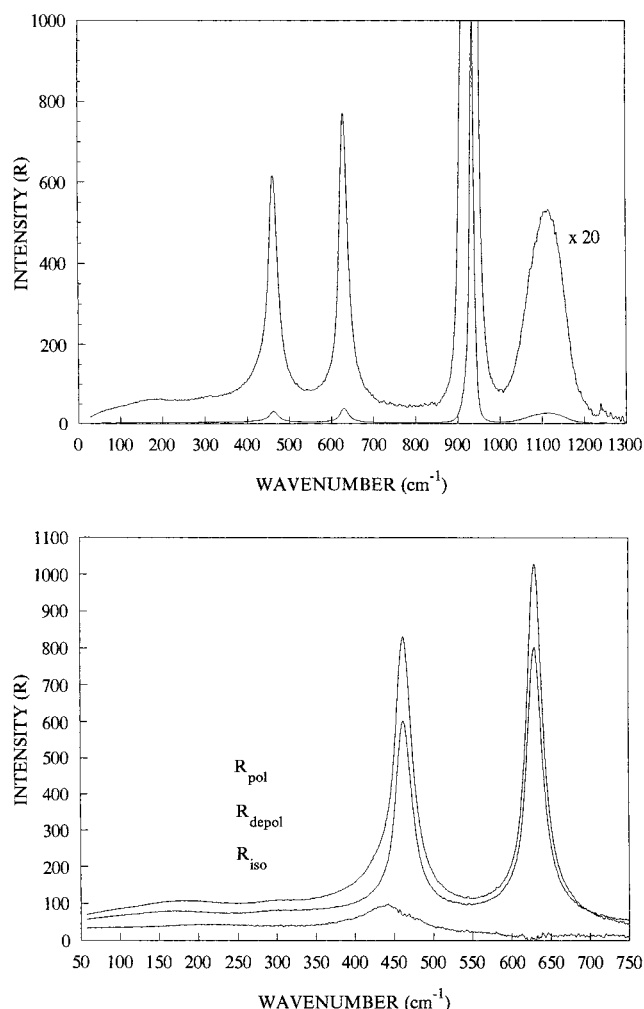


**Figure 1.** (a) Polarized Raman spectrum in R format of a 1.65 M  $\text{Sc}(\text{ClO}_4)_3$  solution in the wavenumber region between 55 and 1300  $\text{cm}^{-1}$  at 25 °C. (b) Raman spectra ( $R_{\text{pol}}$ ,  $R_{\text{depol}}$ , and  $R_{\text{iso}}$ ) of a 1.65 M  $\text{Sc}(\text{ClO}_4)_3$  solution in the wavenumber region between 55 and 750  $\text{cm}^{-1}$  at 25 °C. Note the isotropic component at 442  $\text{cm}^{-1}$ , which has been assigned to  $\nu_1(a_{1g})(\text{ScO}_6)$ , and the depolarized band at 295  $\text{cm}^{-1}$  has been assigned to  $\nu_5(f_{2g})(\text{ScO}_6)$ . The very weak depolarized band at 410  $\text{cm}^{-1}$  has been assigned to  $\nu_2(e_g)(\text{ScO}_6)$ .

$410 \pm 5 \text{ cm}^{-1}$ . These spectroscopic findings are consistent with a hexaaqua Sc(III) ion. The assignment of the  $\text{ScO}_6$  modes were done on the basis of  $O_h$  symmetry ( $\text{H}_2\text{O}$  taken as point mass). The 15 normal modes of the  $\text{ScO}_6$  unit span the representation  $\Gamma_{\text{vib}}(O_h) = a_{1g}(\text{R}) + e_g(\text{R}) + 2f_{1u}(\text{IR}) + f_{2g}(\text{R}) + f_{2u}(\text{n.a.})$ . The modes  $\nu_1(a_{1g})$  (polarized),  $\nu_2(e_g)$ , and  $\nu_5(f_{2g})$  (both depolarized) are Raman active, and the modes  $\nu_3(f_{1u})$  and  $\nu_4(f_{1u})$  are IR active, while the mode  $\nu_6(f_{2u})$  is not observable in solution spectra. The isotropic band at 442  $\text{cm}^{-1}$  can be assigned to  $\nu_1(a_{1g}) \text{ ScO}_6$ , and the depolarized bands at 295 and 410  $\text{cm}^{-1}$  are assigned to  $\nu_5(f_{2g}) \text{ ScO}_6$  and  $\nu_2(e_g)(\text{ScO}_6)$ . The infrared active mode,  $\nu_3(f_{1u})$ , was found to be at 460  $\text{cm}^{-1}$ <sup>132</sup> and confirms the centrosymmetry of  $\text{ScO}_6$ . The frequencies of the  $\text{ScO}_6$  unit and the assignments of the modes are presented in Table 1. The Raman spectrum of the crystalline powder of  $\text{Sc}(\text{ClO}_4)_3 \cdot 6\text{H}_2\text{O}$  at 25 °C reveals a mode at ca. 445  $\text{cm}^{-1}$  and both weak depolarized modes as well. The coincidence of the Raman modes in aqueous solution and in the crystalline powder of  $\text{Sc}(\text{ClO}_4)_3 \cdot 6\text{H}_2\text{O}$  reinforces the existence of the hexaaqua Sc(III)! Finally, we do emphasize that we did not find a polarized mode at 306  $\text{cm}^{-1}$  in  $\text{Sc}(\text{ClO}_4)_3$  solutions but that this mode does occur in  $\text{ScCl}_3$  solutions.



**TABLE 1: ScO<sub>6</sub> Skeleton Modes (ScO<sub>6</sub> Unit Possesses *O<sub>h</sub>* Symmetry) and Raman and IR Spectroscopic Frequencies in Aqueous Sc(ClO<sub>4</sub>)<sub>3</sub> (In ScCl<sub>3</sub>, Sc(NO<sub>3</sub>)<sub>3</sub>, and Sc<sub>2</sub>(SO<sub>4</sub>)<sub>3</sub> Solutions, Complex Formation Occurs)**

assignment and activity	exptl frequencies (cm <sup>-1</sup> ) in H <sub>2</sub> O
$\nu_1(a_{1g})$ Raman	442 ± 1(0.003)
$\nu_2(e_g)$ Raman	410 ± 5 (0.75)
$\nu_3(f_{1u})$ IR	460 ± 5 <sup>a</sup>
$\nu_4(f_{1u})$ IR	not observed
$\nu_5(f_{2g})$ Raman	295 ± 5 (0.75)
$\nu_6(f_{2u})$ ---	not active

<sup>a</sup> Adams, D. M. *Metal-Ligand vibrations and related vibrations*; E. Arnold: London, 1967.

Kanno et al.<sup>3</sup> have interpreted their Raman spectroscopic data by taking into account a heptaqua Sc(III) cluster. A heptaqua Sc(III) cluster with its ScO<sub>7</sub> unit possesses *C<sub>2</sub>* symmetry. The 18 normal modes span the representation  $\Gamma_v(C_2) = 9a$  (Ra, IR) + 9b (Ra, IR). All doubly and triply degenerate modes would lose their degeneracy and split. Certainly, this is not the case! Furthermore, all modes would have to be Raman and infrared active, which is also not observable. We could show, that the mode at 295 cm<sup>-1</sup> is depolarized in Sc(ClO<sub>4</sub>)<sub>3</sub> solution and appears polarized in ScCl<sub>3</sub> solution at 306 cm<sup>-1</sup> (weak chloro complex formation) obscuring the depolarized mode at 295 cm<sup>-1</sup>. The spectra of ScCl<sub>3</sub> will be dealt with in the next section.

The isotropic mode shifts with deuteration of the Sc(ClO<sub>4</sub>)<sub>3</sub> solution to 417 cm<sup>-1</sup> in accordance with the expected isotope shift:

$$\nu_1[(\text{Sc}(\text{OD})_6)^{3+}] = \sqrt{18.02/20.03} \nu_1[(\text{Sc}(\text{OH})_6)^{3+}] = 0.948 \times 442 \text{ cm}^{-1} = 419 \text{ cm}^{-1} \quad (5)$$

Relative intensity measurements for three different Sc(ClO<sub>4</sub>)<sub>3</sub> solutions as a function of concentration (1.65 mol/L, 1.00 mol/L, and 0.5 mol/L) yield a relative scattering coefficient for the  $\nu_1(\text{Sc}-\text{O})$  mode,  $S_h = 0.034 \pm 0.002$ . The perchlorate band,  $\nu_1(a_1)(\text{ClO}_4^-)$  at 935 cm<sup>-1</sup> served as a reference band. The  $S_h$  value is defined as the corrected relative scattering efficiency of the  $[\text{M}(\text{OH})_n]^{m+}$  aqueous metal hydrates. Furthermore,  $S_h$  is defined in the pure isotropic R spectrum. For the  $\nu_1(\text{M}-\text{O})$  modes,  $S_h$  values of 0.02 (Al), 0.12 (Ga), and 0.18 (In) were found, reflecting the increase in the softness of these group IIIa metal ions with an increase in the periodic number. Sc(III), as the first representative of group IIIb metal ions, shows a slightly higher relative molar scattering coefficient than Al(III). This means, in the terminology of inorganic chemistry, Sc(III) is a hard cation.

The Sc<sup>3+</sup> hexaaqua ion may be compared with the well characterized Al<sup>3+</sup> hexaaqua ion<sup>33</sup> in aqueous perchlorate solution. In this solution, the only Al(III) species observable is the  $[\text{Al}(\text{OH})_6]^{3+}$ .<sup>33</sup> A complete vibrational analysis of the  $[\text{Al}(\text{OH})_6]^{3+}$  ion, which can be seen as an "archetypal example of regular octahedral six coordination" (ref 51c, page 143, and section 3.1.), is given in parts a and b of ref 33. The vibrational analysis was carried out taking water as a point mass, so the symmetry of the AlO<sub>6</sub> unit becomes *O<sub>h</sub>*. (The true symmetry of  $[\text{Al}(\text{OH})_6]^{3+}$  cluster is *T<sub>h</sub>*). These spectroscopic findings reveal the structural and spectroscopic similarities between the Al(III) and Sc(III) hexaaqua ions.

These findings are in contrast with the results reported by Kanno et al.<sup>3a</sup> who reported four Raman bands in ScCl<sub>3</sub> and Sc(ClO<sub>4</sub>)<sub>3</sub> solutions and vitreous state at liquid nitrogen temperature. In light of these findings, the question arises: why are there four Raman bands in vitreous ScCl<sub>3</sub> as quoted in ref

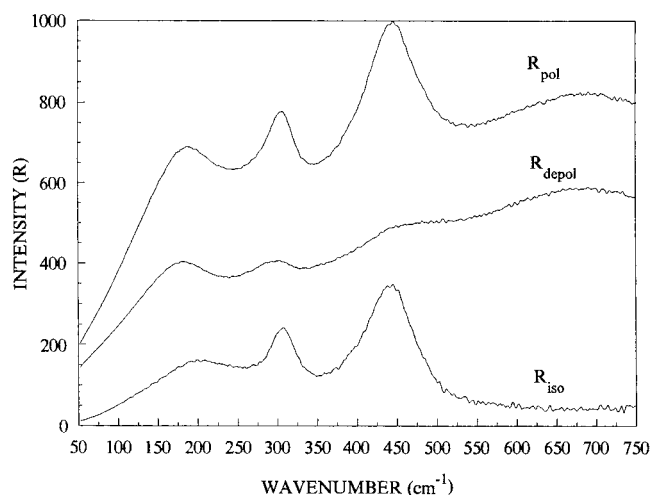


**Figure 2.** Raman spectra ( $R_{\text{pol}}$ ,  $R_{\text{depol}}$ , and  $R_{\text{iso}}$ ) of a 2.55 M ScCl<sub>3</sub><sup>-</sup> solution in the wavenumber region between 55 and 750 cm<sup>-1</sup> at 25 °C.

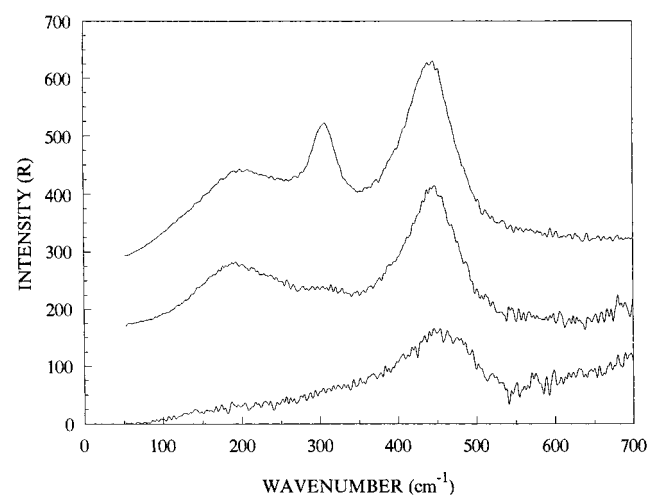


**Figure 3.** Isotropic Raman spectra in R format of a ScCl<sub>3</sub> dilution series: 2.55, 1.55, and 0.255 M ScCl<sub>3</sub><sup>-</sup> solutions from top to bottom at 25 °C.

3a? The answer can be found by inspecting the ScCl<sub>3</sub> solution spectra, which is given below.

**3.1.2. ScCl<sub>3</sub> Solution.** The Raman spectra of a 2.55 M ScCl<sub>3</sub> stock solution at 25 °C is presented in Figure 2. In the isotropic Raman spectrum three bands are observable: at 436 cm<sup>-1</sup> (fwhh = 80 ± 2 cm<sup>-1</sup>), at 306 cm<sup>-1</sup> (fwhh 30 ± 2 cm<sup>-1</sup>), and a weak broad band at 200 cm<sup>-1</sup> (fwhh ca. 120 cm<sup>-1</sup>) representing the intermolecular mode of H-bonded Cl<sup>-</sup> ions of the form H—O—H...Cl<sup>-</sup> (cf. ref 9 and references therein). In addition, the mode at 436 cm<sup>-1</sup> reveals a shoulder at ca. 420 cm<sup>-1</sup>. With dilution of ScCl<sub>3</sub> the band at 306 cm<sup>-1</sup> disappears gradually and in the 0.255 M ScCl<sub>3</sub> solution it is almost gone as can be seen in Figure 3. Therefore, we conclude that the band at 306 cm<sup>-1</sup> is due to a Sc<sup>3+</sup>—Cl<sup>-</sup> stretching mode of  $[\text{Sc}(\text{OH})_{6-n}\text{Cl}_n]^{+(3-n)}$ . The mode at 436 cm<sup>-1</sup> and the shoulder at ca. 425 cm<sup>-1</sup> represent the Sc aqua mode of unligated and ligated Sc(III), respectively. That the stretching mode at 306 cm<sup>-1</sup> is due to Sc<sup>3+</sup>—Cl<sup>-</sup> becomes clear by inspecting a ScCl<sub>3</sub> solution with an excess of LiCl (Sc(III)/Cl(I) = 1:10.4). The isotropic mode at 306 cm<sup>-1</sup> is now dominant, and the mode of the Sc hexaaqua ion,  $\nu_1(\text{ScO}_6)$ , disappeared completely, while a medium strong band at 425 cm<sup>-1</sup> appears, which can be assigned to the vibrations of the remaining water ligands in the mixed Sc chloro water complex, most likely to a mono- or dichloro complex. In the

$\text{ScCl}_3\text{--LiCl}$  mixture with its high chloride content, the  $\text{Sc}^{3+}\text{--Cl}^-$  stretching mode is not frequency shifted compared to the  $\text{ScCl}_3$  solution series, which suggests that the excess in chloride did not result in formation of a  $\text{Sc(III)}$  complex higher in a chloride/scandium ratio (like  $\text{ScCl}_6^{3-}$ , which is known in crystalline form; e.g.  $\text{Cs}_3\text{ScCl}_6^{34}$  or  $\text{ScCl}_3$  and  $\text{ScCl}_4^-$ ).

The same principal findings were made during the course of our Raman spectroscopic studies on electrolyte systems, namely,  $\text{Al(III)}$ ,  $\text{Ga(III)}$ , and  $\text{In(III)}$  perchlorate and chloride aqueous solution. When the counterion is perchlorate, all of the hexaaqua ions are stable. However, when the counterion is chloride, only the  $\text{Al(III)}$  hexaaqua ion is stable. In  $\text{Ga(III)}$  and  $\text{In(III)}$  solutions, chloro complexes are formed.<sup>35</sup> It is known that excess chloride in  $\text{GaCl}_3$  solution results in formation of  $\text{GaCl}_4^-$  from species  $[\text{Ga}(\text{OH}_2)_{6-n}\text{Cl}_n]^{+(3-n)}$  ( $n = 1, 2, 3$ ).<sup>32</sup> The mode,  $\nu_1(\text{GaCl}_4^-)$ , is distinct from the modes,  $\nu_s(\text{Ga}^{3+}\text{--Cl}_n^-)$ , in the  $[\text{Ga}(\text{OH}_2)_{6-n}\text{Cl}_n]^{+(3-n)}$  unit ( $n = 1, 2, 3$ ) species.<sup>35</sup> Obviously, in  $\text{ScCl}_3$  solutions (even with excess of  $\text{Cl}^-$ ) no species such as  $\text{ScCl}_3$ ,  $\text{ScCl}_4^-$ , or  $\text{ScCl}_6^{3-}$  is formed.

The coordination of  $\text{Sc(III)}$  with chloride in aqueous solution was also studied with nonspectroscopic methods initially by Paul<sup>36</sup> and the species  $\text{ScCl}^{2+}$  and  $\text{ScCl}_2^+$  were invoked. For 25 °C and an ionic strength of 0.5 M, the equilibrium quotients for the reactions  $\text{Sc}^{3+} + \text{Cl}^- \rightleftharpoons \text{ScCl}^{2+}$  and  $\text{ScCl}^{2+} + \text{Cl}^- \rightleftharpoons \text{ScCl}_2^+$  were found to be 11.7 and 10.9. Later investigations<sup>37,38</sup> indicated the presence of these species, although the stability constant derived differs considerably from those reported by Paul. Scandium(III) is slightly adsorbed by an anion exchanger column from 7 to 12 M  $\text{HCl}$ , indicating the presence of an anionic species at high chloride concentration.<sup>39</sup> From an ionophoretic investigation, Šmirous et al.<sup>40</sup> invoked the electro neutral  $\text{ScCl}_3$  species and  $\text{ScCl}_4^-$  in  $\text{ScCl}_3$  solutions with an excess of  $\text{Cl}^-$ . It should be mentioned that these physicochemical methods detect besides the inner-sphere complex also complexes of an outer-sphere type. Raman spectroscopy, on the other hand, allows a separate characterization of the inner-sphere complexes. In recent publications by Rudolph et al.,<sup>41</sup> it was shown that in transition metal–sulfate solutions the majority of the complexes are of the outer-sphere type. A recent EXAFS study revealed that chromochloroqua complexes,  $[\text{CrCl}_n(\text{OH}_2)_{6-n}]^{(3-n)+}$  ( $n = 1\text{--}3$ ) form outer-sphere complexes with chloride.<sup>42</sup> The same situation can be invoked in  $\text{ScCl}_3$  solution (inner-sphere, *trans*- $[\text{ScCl}_2(\text{OH}_2)_4]^+$ ; outer-sphere complexes, most probably  $[\text{ScCl}_2(\text{OH}_2)_4]^+\text{Cl}^-$  and  $[\text{ScCl}_2(\text{OH}_2)_4]^+\text{Cl}_2^{2-}$ ). These inner-sphere/outer-sphere complexes would explain the above quoted adsorption experiments on anion exchanger resins quite easily, without invoking negatively charged scandium complexes with a high chloride-to-scandium ratio of the inner-sphere type!

Our spectroscopic results show clearly inner-sphere chloro complex formation in  $\text{ScCl}_3$  solutions. From Raman data and stoichiometric considerations, inner-sphere/outer-sphere complexes can be invoked. These findings are in direct contrast to the findings by Kanno et al.<sup>3</sup> concerning the  $\text{ScCl}_3$  solution spectra and the  $\text{Sc}$  aqua ion assignment. From our spectroscopic findings in  $\text{ScCl}_3$  solution and the findings in  $\text{Sc(III)}$  perchlorate solution it follows that in the perchlorate solution a hexaaqua  $\text{Sc(III)}$  exists. A detailed discussion about the aqueous solution chemistry of  $\text{Sc(III)}$ , its hydration, and complex formation with chloride and sulfate can be found in a recent publication by Rudolph.<sup>43</sup>

### 3.2. Ab initio Molecular Orbital Results. 3.2.1. Structure.

Figure 4 presents the optimized geometries for  $[\text{Sc}(\text{OH}_2)_n]^{3+}$  ( $n = 1\text{--}9$ ) clusters. The structural parameters, including the HF/MP2 energies, are given in Tables 1S–9S of the Supporting

Information.  $\text{Sc(III)}$  water clusters with  $n$  equal to 5, 6, and 7 were described by Åkesson et al.<sup>44</sup> While our results for pentaqua and hexaaqua  $\text{Sc(III)}$  confirm the results in ref 44, the symmetry found for the heptaqua  $\text{Sc(III)}$  structure ( $C_2$ ) deviates from the  $C_{2v}$  structure published in ref 44. The  $C_2$  structure for the heptaqua cluster was also reported by Rotzinger.<sup>45</sup>

The optimized geometries are similar to those structures anticipated on the basis of charge–dipole attractions and water–water repulsions. The single water complex has  $C_{2v}$  symmetry with the water dipole directed toward the  $\text{Sc(III)}$  to enhance the charge–dipole interaction. The water molecules in the larger clusters have their dipoles directed toward the  $\text{Sc(III)}$  and are distributed in highly symmetrical arrangements that tend to minimize water–water repulsion. The  $\text{Sc--O}$  bond lengthens significantly with increasing hydration of the  $\text{Sc(III)}$ . In Figure 5, the calculated  $\text{Sc--O}$  bond lengths are plotted as a function of number of ligands  $n$  located in the first coordination sphere. The geometry of the water ligands changes only slightly with increasing hydration, the  $\text{OH}$  bond lengths are shortening by about 0.02 Å or less and the  $\text{HOH}$  bond angles are increasing of about 1.0°. The optimized geometry of monomeric water is given in Table 2 for comparison.

The linear ( $D_{2d}$ ) and trigonal planar ( $D_3$ ) arrangements of two or three waters around scandium(III) are not necessarily the most thermodynamically stable. For diaqua scandium, the minimum energy structure is bent, with  $C_s$  symmetry, although a  $C_2$  structure was nearly isoenergetic (0.1 kJ) with this structure. These structures are about 13 kJ more stable than the linear  $D_{2d}$  structure. The main difference between the  $C_2$  and  $C_s$  structures is manifested in the change of  $\text{O--Sc--O}$  angle (cf. results given in parts a and b of Table 2S of the Supporting Information). In the  $C_2$  structure, this angle is around 150°, whereas in the  $C_s$  structure, the angle is around 120°. In Table 3S of the Supporting Information, the optimized results for the triaqua  $\text{Sc(III)}$  cluster ( $D_3$ ) are given. For these, the MP2 calculations favor (0.03 kJ) a slightly pyramidal ( $C_3$ ) geometry (deviations of 3° and 7°, respectively, for the angle between  $\text{O--Sc}$  and  $C_3$  axis). This has been noted before<sup>46</sup> and is attributed to the effect of core polarization.

The tetraqua  $\text{Sc(III)}$  cluster possesses  $S_4$  symmetry, and the results are given in Table 4S of the Supporting Information. The pentaqua and hexaaqua  $\text{Sc(III)}$  clusters have  $C_{2v}$  and  $T_h$  symmetry, and their optimized structural parameters are given in Tables 5S and 6S of the Supporting Information. These structures are described in the literature and shall be discussed only briefly. Stable structures for heptaqua and octaqua  $\text{Sc(III)}$  water clusters could be found.  $[\text{Sc}(\text{OH}_2)_7]^{3+}$  possesses  $C_2$  symmetry,  $[\text{Sc}(\text{OH}_2)_8]^{3+}$  possesses  $S_8$  symmetry. We could not find a stable structure for enneaqua  $\text{Sc(III)}$ ,  $[\text{Sc}(\text{OH}_2)_9]^{3+}$ , but we could find a structure with an imaginary  $e$  mode corresponding to water elimination. The structural parameters and the HF/MP2 energies are given in Tables 7S–9S of the Supporting Information. The  $\text{Sc--O}$  bond lengths in the structures with  $n \geq 7$  widen considerably and are, by far, greater than the recently reported experimental  $\text{Sc--O}$  bond length with 2.18 Å.<sup>4</sup>

The results for the ab initio molecular orbital calculations of the hexacoordinated scandium show that the model describes the geometry for aqueous scandium ion. Considering the penta- and heptacoordinated structures, the following conclusions can be drawn. For the pentacoordinated species, the HF/6-31G\* and higher levels all give very similar  $\text{Sc--O}$  distances, with average  $\text{Sc--O}$  distances of 2.146–2.152 Å, and a standard deviation of 0.019–0.020 Å, which are too small when compared with

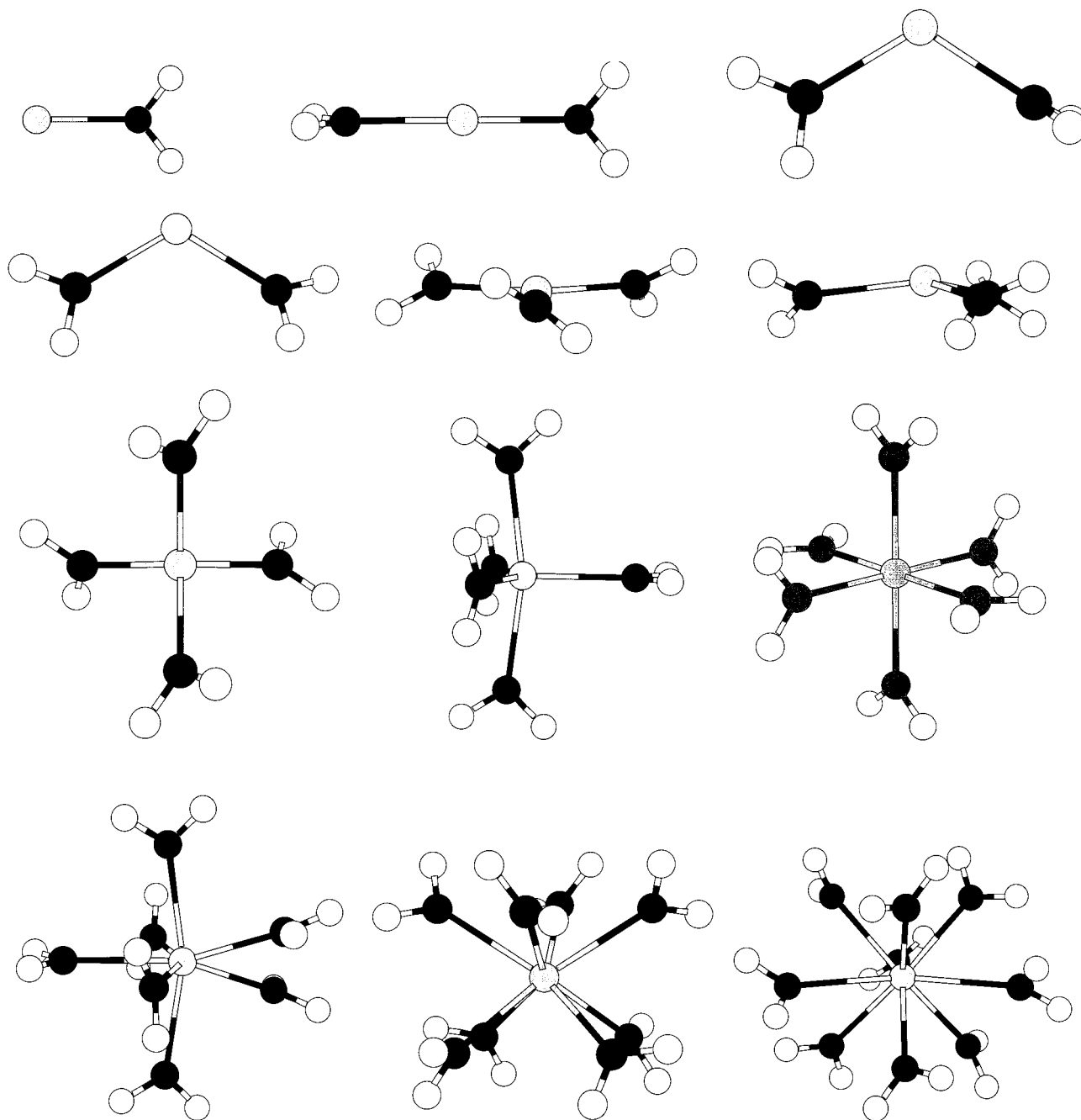


**Figure 4.** Optimized geometries of  $\text{Sc}^{3+}(\text{OH}_2)_n$  ( $n = 1-9$ ) clusters:  $\text{Sc}^{3+}(\text{OH}_2)$  ( $C_{2v}$  sym.);  $\text{Sc}^{3+}(\text{OH}_2)_2$  ( $D_{2d}$ ,  $C_s$ , and  $C_2$  sym.);  $\text{Sc}^{3+}(\text{OH}_2)_3$  ( $D_3$  and  $C_3$  sym.);  $\text{Sc}^{3+}(\text{OH}_2)_4$  ( $S_4$  sym.);  $\text{Sc}^{3+}(\text{OH}_2)_5$  ( $C_{2v}$  sym.);  $\text{Sc}^{3+}(\text{OH}_2)_6$  ( $T_h$  sym.);  $\text{Sc}^{3+}(\text{OH}_2)_7$  ( $C_2$  sym.);  $\text{Sc}^{3+}(\text{OH}_2)_8$  ( $S_8$  sym.);  $\text{Sc}^{3+}(\text{OH}_2)_9$  ( $D_3$  sym.).

the result in ref 4 of  $2.180 \pm 0.007$  Å. These levels of theory also give average Sc–O distances of 2.234–2.242 Å, and a standard deviation of 0.027–0.029 Å, for the heptacoordinated species, which are too large when compared with the experimental Sc–O bond length.

The equilibrium scandium–oxygen distance,  $r_e$ , of 2.181 Å at the HF/6-31G\* level for the  $[\text{Sc}(\text{OH}_2)_6]^{3+}$  (cf. results for hexaaqua Sc(III) in Table 6S of the Supporting Information) is in agreement with the diffraction result of  $2.180 \pm 0.007$  Å.<sup>4</sup> (It has to be noted that diffraction measurements give  $r_a$ , the averaged position of atoms at temperature of experiment, and not  $r_e$ .) These results suggest that the hexaaqua species is the one observed in solution.

It was stated recently that the gas-phase geometries for the  $[\text{Zn}(\text{OH}_2)_6]^{2+}$  cluster are *almost* independent of the solvent effects (second hydration sphere).<sup>20c,47</sup> Therefore, the comparison

of the calculated in vacuo Zn–O bond length with the experimental observed values in aqueous solution should lead to agreement. Furthermore, we could show for a variety of aqua metal ions ( $M = \text{Li}^+$ ,<sup>19</sup>  $\text{Cd}^{2+}$ ,<sup>20a</sup>  $\text{Mg}^{2+}$ ,<sup>20b</sup>  $\text{Zn}^{2+}$ ,<sup>20c</sup> and  $\text{Be}^{2+}$ ,  $\text{Al}^{3+}$ ,  $\text{Ga}^{3+}$ ,  $\text{In}^{3+}$ <sup>48</sup>) that the in vacuo M–O bond lengths reproduce the measured values well. If Sc(III) occurs as an hexaaqua ion, then it follows that the in vacuo Sc–O bond length for the hexaaqua species should be comparable with the EXAFS result, which is true. Therefore, our ab initio calculations demonstrate that the scandium hexaaqua complex ( $T_h$ ) is the stable species (see Figure 4).

**3.2.2. Binding Energies and Enthalpies.** The total binding energies (at 0 K) according to:  $\text{Sc}^{3+} + n\text{H}_2\text{O} \rightleftharpoons [\text{Sc}(\text{OH}_2)_n]^{3+}$  are listed in Table 3. These values were calculated at the HF and MP2 level at the optimized cluster geometries. Table 3 also presents the corresponding binding enthalpies and free energies

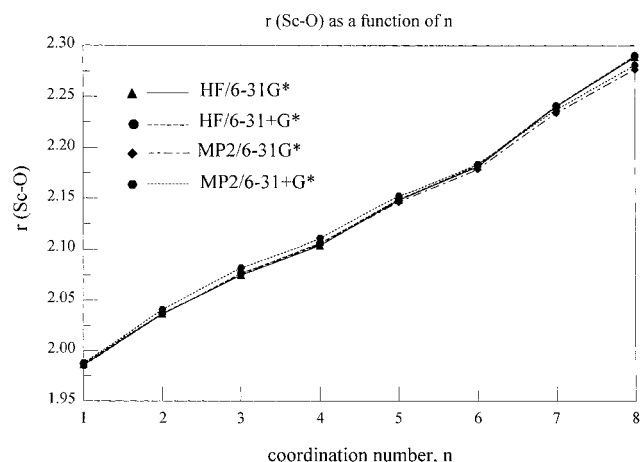


**Figure 5.** Sc–O bond length  $r(\text{Sc-O})$  as a function of the coordination number,  $n$  ( $n = 1-8$ ).

**TABLE 2: Predicted Geometry and HF/MP2 Energy for Monomeric Water<sup>a</sup>**

	H–O bond length (Å)	H–O–H (deg)	energy (au)
HF/6-31G*	0.9473	105.50	−76.0107465
HF/6-31+G*	0.9476	106.52	−76.0177432
MP2/6-31G*	0.9687	103.97	−76.1968478
MP2/6-31+G*	0.9709	105.47	−76.2097766

<sup>a</sup> Geometrical parameters of water determined by microwave spectroscopy: O–H =  $0.9572 \pm 0.0003$  Å; HOH =  $104^\circ 31' \pm 3'$  (taken from: Benedict, W. S.; Gailar, N.; Plyler, E. K. *J. Chem. Phys.* **1956**, *24*, 1139).

at 298.15 K. The incremental binding energy, enthalpy, and Gibbs free energy values are given in Table 4. For the MP2/6-31+G\* level, the incremental binding enthalpies at 298.15 K, as a function of coordination number, are presented in Figure 6. The trends seen for the incremental binding enthalpies are in accordance with those anticipated from electrostatic considerations. The Sc(III)–water interaction weakens with increasing coordination of the metal. This trend arises from the repulsion of the dipoles between the water ligands and from unfavorable many body interactions. Figure 6 also shows that the incremental binding enthalpies diminish rather smoothly with increasing  $n$ , the coordination number. Between 6 and 7, a rather sudden step occurs, indicating the relative strength of the hexaqua Sc(III) cluster.

For aqueous clusters with  $n \geq 2$ , several distinct equilibrium structures for a fixed cluster size are possible. For example, for  $[\text{K}(\text{OH}_2)_4]^+$ , three optimized structures were established having binding energies within about 4 kJ/mol of each other.<sup>46</sup> Besides two inner-sphere clusters (all four water ligands in the first coordination sphere; symmetry  $S_4$  and  $C_4$ ), a third cluster, denoted  $\text{K}[3+1]$ , having only three inner-sphere waters and the fourth water in the second hydration sphere forming H-bonds with water molecules in the first sphere. It was found that the latter structure was more stable than the  $S_4$  and  $C_4$  structures by 1.7 and 3.8 kJ/mol, respectively (MP2/6-31+G\* level). In general it was found that “ $n + m$ ” clusters with at least one water molecule in the second hydration sphere are more stable than those with all waters in the first hydration sphere when the incremental binding energy is less than 50–59 kJ/mol. When the energy for placing an additional water in the first hydration sphere is less than this threshold, it becomes more favorable for that molecule to remain in the second hydration shell, forming two hydrogen bonds worth about 25 kJ/mol. The binding enthalpy of the hexaqua cluster is between 54% and 60% of the experimental hydration enthalpy of  $\text{Sc}^{3+}$ .

**TABLE 3: Binding Energies (at 0 K), Enthalpies (298.15 K), and Free Energies (at 298.15 K) in kJ/mol of  $\text{Sc}(\text{OH}_2)_n^{3+}$  ( $n = 1-9$ ) Clusters<sup>b</sup>**

$n$	HF/6-31G*	MP2/6-31G*	HF/6-31+G*	MP2/6-31+G*
Binding Energies <sup>a</sup>				
1	−557.99	−596.44	−542.51	−567.50
2	−1021.82	−1079.87	−991.20	−1024.27
3	−1426.55	−1499.17	−1381.18	−1418.78
4	−1778.57	−1865.10	−1720.67	−1763.51
5	−2047.12	−2146.67	−1979.70	−2031.90
6	−2292.45	−2406.03	−2217.64	−2281.35
7	−2428.65	−2558.48	−2343.43	−2423.95
8	−2558.76	−2705.92	−2466.30	−2567.07
9	−2629.49	−2793.52	−2530.73	−2649.42
Enthalpies				
1	−550.67	−590.26	−535.00	−560.84
2	−1010.47	−1067.17	−976.97	−1010.71
3	−1405.38	−1479.15	−1359.49	−1397.61
4	−1741.92	−1837.06	−1683.31	−1733.98
5	−1993.35	−2101.64	−1924.94	−1985.15
6	−2222.32	−2344.95	−2146.31	−2218.40
7	−2341.09	−2480.68	−2254.94	(−2344.55)
8	−2454.50	(−2611.42)	−2356.60	(−2466.46)
9	−2515.80	(−2689.59)	−2411.78	(−2539.56)
Free Energies				
1	−519.84	−559.42	−504.18	−530.03
2	−941.76	−1008.83	−916.05	−950.78
3	−1304.66	−1381.20	−1259.98	−1297.87
4	−1598.49	−1693.05	−1540.58	−1591.52
5	−1803.31	−1911.36	−1733.75	−1794.13
6	−1980.17	−2103.46	−1902.60	−1975.35
7	−2059.33	−2200.35	−1973.48	(−2064.52)
8	−2124.22	(−2282.57)	−2026.46	(−2137.75)
9	−2139.91	(−2315.13)	−2035.68	(−2164.89)

<sup>a</sup> The binding energies are not corrected for BSSE. Calculating the BSSE contribution is likely unnecessary for basis sets with diffuse functions, for two reasons. First, the added function describes the regions far from the nucleus, where BSSE arises. Second, although centered at particular nuclei, the diffuse function cannot be considered as “belonging” to that nucleus since it primarily describes regions of space that may actually be closer to other nuclei, and thus the usual partitioning of the atomic centers may be rendered invalid. The difference between the 6-31G\* and 6-31+G\* results may be regarded as being mostly due to BSSE, warranting the inclusion of the former. <sup>b</sup> Values in parentheses derived from vibrational corrections as obtained from the corresponding Hartree–Fock calculation.

Scandium water clusters should undergo similar behavior, although the H-bonds in this trivalent metal ion cluster should be much stronger. In particular, the stability of the heptaqua Sc(III) cluster,  $[\text{Sc}(\text{OH}_2)_7]^{3+}$ , denoted  $\text{Sc}[7+0]$  proposed by Yamaguchi et al., relative to the cluster  $[\text{Sc}(\text{OH}_2)_6]^{3+}(\text{OH}_2)$ , denoted  $\text{Sc}[6+1]$ , where one of the waters is placed in the second sphere, needs to be addressed. The optimized structure  $[6+1]$  demonstrates the formation of two strong H-bonds between the first sphere and the second sphere water. The calculated thermodynamics of the reaction  $[\text{Sc}(\text{OH}_2)_7]^{3+} \rightarrow [\text{Sc}(\text{OH}_2)_6]^{3+}(\text{OH}_2)$  is given in Table 5. For weaker interactions, basis set superposition error (BSSE) can become a problem for calculating the interaction energies. The effects of BSSE have been investigated for the  $\text{Sc}[6+1]$  and  $\text{Sc}[7+0]$  clusters, and the following points should be made (cf. Table 10S of the Supporting Information). The BSSE content of the interaction between the second sphere water and the hexaqua units of  $\text{Sc}[6+1]$  can be as large as 20 kJ/mol/water in the  $[6+1]$  structure, but is even more important in the compact  $[7+0]$  cluster. The difference in BSSE content is about 5–15 kJ/mol. Because the difference in energy between the  $[6+1]$  and  $[7+0]$  is small, a BSSE correction of ca. 10 kJ/mol makes a big difference. The BSSE correction strengthens our case for the hexacoordinated

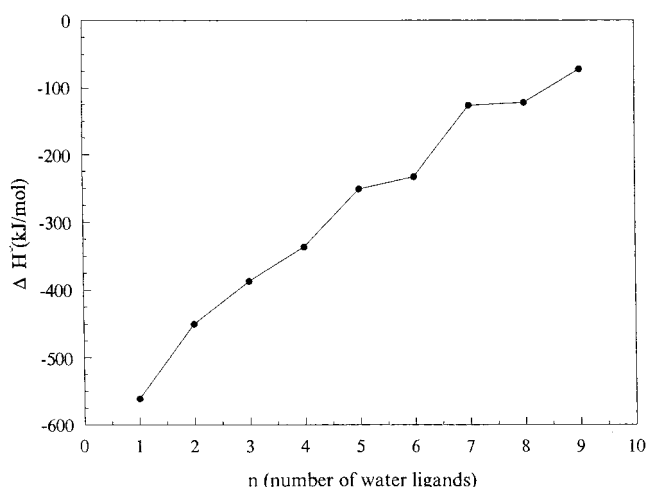


**TABLE 4: Incremental Binding Energies (0 K), Enthalpies (298.15 K), and  $\Delta G^\circ$  Values (298.15 K) for the Formation of First-Sphere Sc(III) Water Clusters ( $n = 1-9$ )**

	$\Delta E(0\text{ K})$	$\Delta H^\circ(298.15\text{ K})$	$\Delta G^\circ(298.15\text{ K})$
$\text{Sc}^{3+} + \text{H}_2\text{O} = \text{Sc}(\text{OH}_2)^{3+}$			
HF/6-31G*	-557.99	-550.67	-519.84
HF/6-31+G*	-542.51	-535	-504.18
MP2/6-31G*	-596.44	-590.26	-559.42
MP2/6-31+G*	-567.5	-560.84	-530.03
$\text{Sc}(\text{OH}_2)^{3+} + \text{H}_2\text{O} = \text{Sc}(\text{OH}_2)_2^{3+}$			
HF/6-31G*	-463.83	-459.80	-421.92
HF/6-31+G*	-448.69	-441.97	-411.87
MP2/6-31G*	-483.43	-476.91	-449.41
MP2/6-31+G*	-456.77	-449.87	-420.75
$\text{Sc}(\text{OH}_2)_2^{3+} + \text{H}_2\text{O} = \text{Sc}(\text{OH}_2)_3^{3+}$			
HF/6-31G*	-404.73	-394.91	-362.90
HF/6-31+G*	-389.98	-382.52	-343.93
MP2/6-31G*	-419.30	-411.98	-372.37
MP2/6-31+G*	-394.51	-386.90	-347.09
$\text{Sc}(\text{OH}_2)_3^{3+} + \text{H}_2\text{O} = \text{Sc}(\text{OH}_2)_4^{3+}$			
HF/6-31G*	-352.02	-336.54	-293.83
HF/6-31+G*	-339.49	-323.82	-280.6
MP2/6-31G*	-365.93	-357.91	-311.85
MP2/6-31+G*	-344.73	-336.37	-293.65
$\text{Sc}(\text{OH}_2)_4^{3+} + \text{H}_2\text{O} = \text{Sc}(\text{OH}_2)_5^{3+}$			
HF/6-31G*	-268.55	-251.43	-204.82
HF/6-31+G*	-259.03	-241.63	-193.17
MP2/6-31G*	-281.57	-264.58	-218.31
MP2/6-31+G*	-268.39	-251.17	-202.61
$\text{Sc}(\text{OH}_2)_5^{3+} + \text{H}_2\text{O} = \text{Sc}(\text{OH}_2)_6^{3+}$			
HF/6-31G*	-245.33	-228.97	-176.86
HF/6-31+G*	-237.94	-221.37	-168.85
MP2/6-31G*	-259.36	-243.31	-192.1
MP2/6-31+G*	-249.45	-233.25	-181.22
$\text{Sc}(\text{OH}_2)_6^{3+} + \text{H}_2\text{O} = \text{Sc}(\text{OH}_2)_7^{3+}$			
HF/6-31G*	-136.2	-118.77	-79.16
HF/6-31+G*	-125.79	-108.63	-70.88
MP2/6-31G*	-152.45	-135.73	-96.8
MP2/6-31+G*	-142.6	-126.15	-89.17
$\text{Sc}(\text{OH}_2)_7^{3+} + \text{H}_2\text{O} = \text{Sc}(\text{OH}_2)_8^{3+}$			
HF/6-31G*	-130.11	-113.41	-64.89
HF/6-31+G*	-122.87	-101.66	52.98
MP2/6-31G*	-147.44	-130.74	-82.22
MP2/6-31+G*	-143.12	-121.91	-73.23
$\text{Sc}(\text{OH}_2)_8^{3+} + \text{H}_2\text{O} = \text{Sc}(\text{OH}_2)_9^{3+}$			
HF/6-31G*	-70.73	-61.3	-15.69
HF/6-31+G*	-64.43	-55.18	-9.22
MP2/6-31G*	-87.60	-78.17	-32.56
MP2/6-31+G*	-82.35	-73.10	-27.14

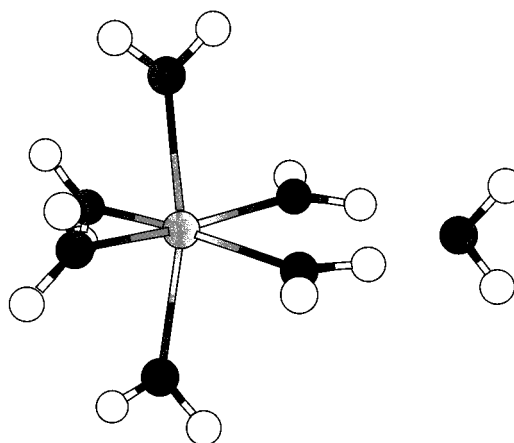
species, since BSSE destabilizes the [7+0] structure relative to the [6+1]. The uncorrected interaction energies of  $\text{Sc}[7+0]$  relative to  $\text{Sc}[6+1]$  are -9.46, -18.58, -7.41, -12.14 kJ/mol at the HF/6-31G\*, HF/6-31+G\*, MP2/6-31G\*, and MP2/6-31+G\* levels, respectively. The BSSE corrected values are -16.36, -31.81, -11.37, and -19.99 kJ/mol, respectively. The preferred hexacoordinated structure with the seventh water molecule in the outer sphere is given in Figure 7. The BSSE uncorrected and corrected thermodynamic values of the reaction  $[\text{Sc}(\text{OH}_2)_7]^{3+} \rightarrow [\text{Sc}(\text{OH}_2)_6]^{3+}(\text{OH}_2)$  are given together in Table 5. For the clusters  $\text{Sc}[7+0]$  and  $\text{Sc}[6+1]$ , the interaction, deformation, uncorrected and corrected binding energies, and BSSE contents are given along with the relevant energies for the reaction in Table 10S of the Supporting Information.

Clearly, the reaction  $\text{Sc}[7+0] \rightarrow \text{Sc}[6+1]$  is energetically favored and evidence for the stability of the hexaaqua Sc(III). A more general statement can be formulated. As the Sc(III)-water complex grows in size, the Sc-O interaction becomes weaker because of both decreasing net charge on scandium and

**Figure 6.** Incremental binding enthalpies (MP2/6-31+G\* basis) at 298.15 K as a function of  $n$ , the number of water ligands, in the first hydration sphere.**TABLE 5: Difference in SCF Energy  $\Delta E_b$  (0 K),  $\Delta H^\circ$  (298.15 K), and  $\Delta G^\circ$  (298.15 K) for  $\text{Sc}[6+1]$  and  $\text{Sc}[7+0]$  When One Water Moves from First Hydration Sphere to Second Hydration Sphere<sup>a</sup>**

level	$\Delta E_b$ (kJ/mol)	$\Delta H^\circ$ (kJ/mol)	$\Delta G^\circ$ (kJ/mol)
HF/6-31G(d) uncorrected	-9.46	-10.44	-14.35
corrected	-16.36	-17.32	-21.23
MP2/6-31G(d) uncorrected	-18.58	-19.14	-20.45
corrected	-31.81	-32.98	-34.30
HF/6-31+G(d) uncorrected	-7.41	-8.76	-13.84
corrected	-11.37	-12.72	-17.80
MP2/6-31+G(d) uncorrected	-12.14	-13.69 <sup>b</sup>	-15.50
corrected	-19.99	-21.55 <sup>b</sup>	-23.36

<sup>a</sup> The values are BSSE uncorrected, and in the second line the corrected values are given. <sup>b</sup> Vibrational contribution calculated from additivity principle as  $\Delta E_{\text{thermal}}(\text{MP2/6-31+G}^*) = \text{MP2/6-31+G}^* - \text{HF/6-31+G}^* - \text{HF/6-31G}^*$

**Figure 7.** Structural model (symmetry  $C_2$ ) of the  $[\text{Sc}(\text{H}_2\text{O})_6(\text{OH}_2)]^{3+}$  cluster.

of water-water repulsion in the first hydration sphere. However, a water molecule in the second hydration sphere can form strong hydrogen bond(s) to the first hydration sphere because of the polarizing effect of the cation. Thus, eventually it is energetically preferable for water to remain in the second hydration sphere as opposed to squeezing into the first hydration sphere as the number of waters grows. For scandium, it appears as though the seventh water molecule prefers to stay in the second sphere. Rotzinger<sup>45</sup> has shown computationally that the Sc(III) hexaaqua

**TABLE 6: Sc–O Symmetric Stretching Frequency of  $\text{Sc}(\text{OH}_2)_n^{3+}$  Clusters as a Function of Hydration Number,  $N$ , the Coordination Number of the First Hydration Sphere**

$n$ (coordination number)	HF/6-31G*	MP2/6-31G*	HF/6-31+G*	MP2/6-31+G*
1	611	613	607	605
2	536	538	532	530
3	462	462	458	457
4	440	440	437	432
5	419	419	417	413
6	398	398	396	394
7	385	394	389	
8	350		349	
9	344		347	

ion undergoes associative exchange (A), with the intermediate possessing symmetry  $C_2$ .

We have verified the existence of this intermediate (our  $\text{ScAq7 [7+0]}$  structure). Our attempts to generate an intermediate of higher symmetry ( $C_{2v}$ ) gave a second-order saddle point, although this symmetry was proposed by Åkesson et al.<sup>44</sup> as a minimum structure. Our energy difference between the  $[7+0]$  and  $[6+1]$  is much greater than the value given by Rotzinger<sup>45</sup> (0.5 kJ/mol) who did not include diffuse functions or correlation energy in his treatment. We used the more stable isomer for the  $[6+1]$  species in which the second-sphere water bridges two waters of the first hydration sphere.

**3.2.3. Frequency Calculations and the Modeling of the  $[\text{Sc}(\text{OH}_2)_{18}]^{3+}$  Cluster.** The tendency of the  $\nu_1(\text{ScO}_n)$  frequencies of the  $[\text{Sc}(\text{OH}_2)_n]^{3+}$  water clusters ( $n = 1-9$ ) shows that the frequencies fall constantly with an increase in coordination number,  $n$ . In Table 6, we present these  $\nu_1(\text{ScO}_n)$  frequencies of the corresponding  $[\text{Sc}(\text{OH}_2)_n]^{3+}$ . A comparison of calculated and experimental bond lengths and binding enthalpies suggests that the hexaaqua Sc(III) water cluster, denoted  $\text{Sc}[6+0]$ , will be the preferred ion in aqueous solution. The frequencies for this hexaaqua Sc(III) cluster are given in Table 7. For comparison, the frequencies for monomeric water for the four relevant levels of theory/basis sets are given in Table 8. The striking features by comparing the modes of the “free” water molecules,  $\nu_2(\text{H}_2\text{O})$ ,  $\nu_1(\text{H}_2\text{O})$ , and  $\nu_3(\text{H}_2\text{O})$  with the modes in the hexaaqua Sc(III) cluster ion are that the stretching vibrations of water shift to lower wavenumbers upon coordination, whilst the deformation mode shifts to higher wavenumbers upon coordination. The calculated  $\nu_1(\text{ScO}_6)$  frequency (HF/6-31G\*) however, is almost  $45 \text{ cm}^{-1}$  (ca. 11%) smaller than the observed symmetric stretching mode,  $\nu_1(\text{ScO}_6)$  at  $442 \text{ cm}^{-1}$ . We could show for  $\text{Li(I)}$ ,<sup>19</sup>  $\text{Cd(II)}$ ,<sup>20a</sup>  $\text{Mg(II)}$ ,<sup>20b</sup> and  $\text{Zn}^{20c}$  that this poor agreement was not due to a deficiency of the theory (such as an inadequate basis set or neglect of correlation). The HF/6-31G\* basis set is usually sufficient for describing geometries and (scaled) frequencies. The extension of the basis set was examined in order to rule out this possibility for Sc(III). The addition of diffuse functions to oxygen increases the Sc–O distance by almost  $0.0013 \text{ Å}$  and slightly decreases the frequency of  $\nu_1(\text{ScO}_6)$  to  $396 \text{ cm}^{-1}$ . The effect of correlation was then ascertained by performing MP2/6-31G\* and MP2/6-31+G\* calculations. The Sc–O bond changes to  $2.179$  and  $2.183 \text{ Å}$ , respectively. Considering our best values,  $\nu_1(\text{ScO}_6)$ , the total symmetric stretching frequency of the hexaaqua complex is still underestimated. Anharmonicity of the bond is unlikely to account for such a big deviation.<sup>49</sup> Clearly, the theory is not to blame. The only conclusion reachable from the above data is that the cluster model used to calculate the frequencies is insufficient. The six water molecules represent only the first hydration shell. In solution, these water molecules form strong H-bonds with water molecules in the second hydration shell

because of the strong polarizing effect of the scandium ion. Obtaining a more accurate  $\nu_1(\text{ScO}_6)$  frequency necessitates the inclusion of an explicit second solvation sphere in the ab initio calculation, as was shown recently for  $\text{Li}$ ,<sup>19</sup>  $\text{Cd}^{2+}$ ,<sup>20a</sup>  $\text{Zn}^{2+}$ ,<sup>20c</sup>  $\text{Mg}^{2+}$ ,<sup>20b</sup> and also for  $\text{Be}^{2+}$ ,  $\text{Al}^{3+}$ ,  $\text{Ga}^{3+}$ , and  $\text{In}^{3+}$ .<sup>48</sup> The existence of the second hydration sphere was established for other trivalent metal ions, as was established recently by EXAFS in Cr(III), Ga(III), and Rh(III) (and Zn(II)).<sup>50</sup>

**The  $\text{Sc}^{3+}(\text{OH}_2)_{18}$  Cluster.** The calculated  $[\text{Sc}(\text{OH}_2)_{18}]^{3+}$  cluster, denoted  $\text{Sc}[6+12]$ , corresponds to the local minimum with  $T$  symmetry. Structural parameters calculated at the HF/3-21G, HF/6-31G\*, and HF/6-31+G\* are given in Table 9. The Sc–O distances for  $\text{Sc}[6+0]$  are  $2.126 \text{ Å}$ ,  $2.179 \text{ Å}$ , and  $2.183 \text{ Å}$  at the HF/3-21G, HF/6-31G\*, and HF/6-31+G\* levels, respectively. For  $\text{Sc}[6+12]$ , the corresponding distances (bond length between Sc(III) and the oxygen of the first-sphere water,  $\text{Sc}-\text{O}_{\text{first-sphere}}$ ) are  $2.101$ ,  $2.150$ , and  $2.151 \text{ Å}$ , respectively, a shortening of about  $0.03 \text{ Å}$ . For the latter species, the Sc–O distances between Sc(III) and the oxygen of the second sphere ( $\text{Sc}-\text{O}_{\text{second-sphere}}$ ) are  $4.098$ ,  $4.297$ , and  $4.319 \text{ Å}$ , respectively. These  $\text{Sc}-\text{O}_{\text{second-sphere}}$  bond lengths are primarily determined by the H-bond distances between water molecules of the first- and second-sphere of  $1.652$ ,  $1.796$ , and  $1.814 \text{ Å}$ , respectively. These results illustrate the inadequacy of the HF/3-21G basis set, which overestimates the strength of the H-bonds.<sup>49</sup> The H-bond in water dimers is  $1.825 \text{ Å}$  (HF/3-21G),  $2.026 \text{ Å}$  (HF/6-31G\*), and  $2.014 \text{ Å}$  (HF/6-31+G\*).<sup>20b</sup> The short H-bond distances in the  $\text{Sc}[6+12]$  cluster demonstrate further the formation of strong H-bonds. The slight decrease in Sc–O distance in the first hydration sphere of the cluster arises because the water molecules in the second-sphere polarize the waters in the first shell, so that the interaction of  $\text{Sc}^{3+}$  and the first-shell water molecules is enhanced. Although the HF/6-31+G\* geometries are very similar to the HF/6-31G\* results, the energies are much improved, since the addition of diffuse functions should partially eliminate basis set superposition error (BSSE). The results for the binding energies are shown in the paragraph below.

The structural model of the  $[\text{Sc}(\text{H}_2\text{O})_{18}]^{3+}$  cluster is given in Figure 8. The octadecaaqua scandium(III) cluster (of symmetry  $T$ ) corresponds to our structure C in ref 20b. It should be noted that during the course of our optimization of  $\text{Mg}[6+12]$ , two other structures, denoted as A and B, with symmetry  $T_h$  were found (cf. Pye and Rudolph, in ref 20b). However, neither of these structures represented an energy minimum. Our results call, therefore, the structure of the similar octadecaaqua metal ion published recently by Siegbahn and co-workers<sup>51</sup> into question. The structure published by Siegbahn et al.<sup>51</sup> corresponds with our nonequilibrium structure B.

The  $\nu_1(\text{ScO}_6)$  frequency, equal to  $447 \text{ cm}^{-1}$  (HF/6-31G\* level) reproduces the measured frequency much better. The (unscaled) predicted frequencies for the  $[\text{Sc}(\text{OH}_2)_{18}]^{3+}$ ,  $\text{Sc}[6+12]$  cluster at the HF/6-31G\* level are given in Table 10. The 159 normal modes span the representation  $\Gamma_{\text{vib}}(T) = 13a(R) + 13e(R) + 40f(IR, R)$ . The assignments as well as the normal modes are also given in Table 9. In some cases, the  $\text{Sc}-\text{O}_6$  modes ( $\Gamma_{\text{vib}}(T) \text{ ScO}_6 = a(R) + e(R) + 4f(IR, R)$ ) couple strongly with either librational modes of the second-sphere water molecules or restricted translational modes. Compared to our gas-phase cluster model, in real solutions the symmetry allowed coupling would not be as severe. In any case, the stretching modes  $\nu_1(\text{ScO}_6)$  at  $447 \text{ cm}^{-1}$  (a mode) and  $\nu_3(\text{ScO}_6)$  at  $495 \text{ cm}^{-1}$  (f mode) and the modes  $\nu_2(\text{ScO}_6)$  at  $421 \text{ cm}^{-1}$  and  $\nu_5(\text{ScO}_6)$  at  $271 \text{ cm}^{-1}$  (e and f mode) are unambigu-

**TABLE 7: Unscaled Frequencies (in  $\text{cm}^{-1}$ ), Intensities, and Force Constants of the Modes of the Hexaaqua Sc(III) Ion:  $\Gamma_{\text{vib}} = 3A_g(\text{R,tp}) + a_u(\text{n.a.}) + 3E_g(\text{R,dp}) + E_u(\text{n.a.}) + 5f_g(\text{R,dp}) + 8f_u(\text{IR})^a$** 

HF/6-31-G* <sup>b</sup>			HF/6-31+G* <sup>b</sup>			MP2/6-31G* <sup>b</sup>			MP2/6-31+G* <sup>b</sup>			mode	activity
freq	<i>I</i>	f.c.	freq	<i>I</i>	f.c.	freq	<i>I</i>	f.c.	freq	<i>I</i>	f.c.		
88.6	0.98	0.021	91.5	0.775	0.022	88.2	1.266	0.0206	90.9	1.125	0.0219	$\delta \text{O}-\text{Sc}-\text{O}(\text{f}_u)$	IR
134.7	0.43	0.049	139.5	0.457	0.052	129.5		0.0455	134.5		0.0489	$\delta \text{O}-\text{Sc}-\text{O}(\text{f}_g)$	Raman
141.0	0.16	0.06	142.2	0.12	0.060	138.3	0.06	0.057	138.9	0.1134	0.0575	$\delta \text{O}-\text{Sc}-\text{O}(\text{f}_u)$	IR
216.4		0.028	236.9		0.033	221.7		0.029	226.6		0.029	$\tau \text{HOH}(\text{e}_u)$	n.a.
294.2	2.05	0.052	311.6	0.713	0.058	301.8		0.055	307.6		0.0566	$\tau \text{HOH}(\text{f}_g)$	Raman
348.8	0.027	0.425	348.3	0.0008	0.423	354.4		0.438	351.14		0.430	$\nu_{\text{as}}\text{Sc}-\text{O}(\text{e}_g)$	Raman
397.1	0.71	0.556	396.5	1.11	0.554	398		0.562	394.4		0.553	$\nu_s \text{Sc}-\text{O}(\text{a}_g)$	Raman
416.5		0.103	432.1		0.111	426.7		0.108	438.5		0.114	$\tau \text{HOH}(\text{a}_u)$	n.a.
435.2	7.26	0.720	433.1	9.62	0.722	438.5	1.435	0.628	433.4	4.369	0.644	$\nu_{\text{as}}\text{Sc}-\text{O}(\text{f}_u)$	IR
580.4	1.94	0.228	592.9	1.626	0.238	532.3		0.192	547.2		0.203	$\omega \text{HOH}(\text{f}_g)$	Raman
613.6	263	0.260	622	212	0.264	562.7	335	0.216	570.2	321	0.222	$\omega \text{HOH}(\text{f}_u)$	IR
689.4	0.363	0.322	693.6	0.137	0.327	644.5		0.281	648.5		0.286	$\rho \text{HOH}(\text{f}_g)$	Raman
695.3	849	0.353	699.6	846	0.357	655.1	709	0.323	659.4	657	0.324	$\rho \text{HOH}(\text{f}_u)$	IR
1842.5	362	2.170	1839.5	362	2.164	1737.3	314	1.932	1728.6	320	1.912	$\delta \text{HOH}(\text{f}_u)$	IR
1843.2	4.51	2.172	1840.8	3.23	2.167	1738.4		1.934	1730.3		1.916	$\delta \text{HOH}(\text{e}_g)$	Raman
1851.4	0.172	2.183	1848.1	0.017	2.175	1746.4		1.942	1737.4		1.921	$\delta \text{HOH}(\text{a}_g)$	Raman
3887.8	41	9.31	3884.4	35	9.293	3618.7		8.060	3589.6		7.931	$\nu_s \text{OH}(\text{e}_g)$	Raman
3891	675	9.327	3887.3	628	9.308	3621.6	634	8.074	3591.9	579	7.943	$\nu_s \text{OH}(\text{f}_u)$	IR
3913.7	242	9.453	3908	287	9.424	3743.2		8.185	3610		8.036	$\nu_s \text{OH}(\text{a}_g)$	Raman
3953.4	55.8	9.985	3954	45.4	9.988	3694.6		8.712	3670.8		8.60	$\nu_{\text{as}}\text{OH}(\text{f}_g)$	Raman
3954.5	768	9.992	3955	736	9.994	3695.5	665	8.717	3671.5	644.5	8.604	$\nu_{\text{as}}\text{OH}(\text{f}_u)$	IR

<sup>a</sup> R = Raman active with tp = totally polarized and dp = depolarized; IR = infrared active; n.a. = mode not allowed. <sup>b</sup> For each individual basis set/level of theory, the IR activities ( $\text{km/mol}$ ) and the Raman intensities ( $\text{\AA}^4/\text{au}$ ) are given (because of the mutual exclusion rule only modes with subscript g are Raman active and modes with subscript u are IR active). In the third column, the force constants ( $\text{mdyn/\AA}$ ) are given. At the MP2 level, only the IR intensities are given ( $\text{km/mol}$ ) together with the force constants ( $\text{mdyn/\AA}$ ); no Raman activities were obtained at this level.

**TABLE 8: Predicted Harmonic Frequencies ( $\text{cm}^{-1}$ ) and in Brackets the IR ( $\text{km/mol}$ ) and Raman ( $\text{\AA}^4/\text{amu}$ ) Intensities of Water<sup>a</sup>**

mode	HF/6-31G*				HF/6-31+G*				MP2/6-31G*			MP2/6-31+G*		
	freq	IR	R	f.c.	freq	IR	R	f.c.	freq	IR	f.c.	freq	IR	f.c.
$\nu_3(\text{b}_2)$	4188.7	5.1	39.1	11.19	4190.2	58.1	39.1	11.21	3916.2	38.7	9.77	3893.6	70.5	9.67
$\nu_1(\text{a}_1)$	4070.4	18.2	75.5	10.21	4071.1	23.4	74.8	10.20	3774.8	5.5	8.77	3747.9	11.6	8.64
$\nu_2(\text{a}_1)$	1826.5	107	5.7	2.13	1796.6	119	3.0	2.06	1735.5	88.6	1.92	1681.8	106	1.81

<sup>a</sup> Note that the MP2 frequencies reproduce the harmonic experimental frequencies quite well, while the frequencies at the HF level are by ca. 10% too high. Experimental frequencies for water are 3756, 3657, and  $1595 \text{ cm}^{-1}$  and their harmonic values are 3943, 3832, and  $1649 \text{ cm}^{-1}$ . The data are taken from the following: Hoy, A. R.; Mills, I. M.; Strey, G. *Mol. Phys.* **1972**, *24*, 1265.

**TABLE 9: Structural Parameters, Energy (Hartree), and Thermodynamic Parameters ( $\Delta E_{\text{B}}$ , binding energy, at 0 K and  $\Delta H^\circ$ , the enthalpy of the cluster formation at 298.15 K) Calculated for the  $\text{Sc}(\text{OH}_2)_{18}^{3+}$  Cluster Denoted Sc[6+12]**

	HF/3-21G	HF/6-31G*	HF/6-31+G*
Bond Length (in $\text{\AA}$ )			
Sc-O (first water sphere)	2.101	2.150	2.151
Sc-O (second water sphere)	4.098	4.297	4.319
O-H (first water sphere)	0.993	0.971	0.970
O-H(A) (second water sphere)	0.968	0.953	0.953
O-H(B) (second water sphere)	0.982	0.955	0.955
HO1...H bond length	1.652	1.796	1.814
Angle $\Theta$ (deg)			
HOH angle (first water sphere)	112.1	108.4	108.3
HOH angle (second water sphere)	112.0	106.9	106.9
energy (hartree)	-2116.897313	-2127.553817	-2127.616197
$\Delta E_{\text{B}}$ (0 K) (kJ/mol)	-4821.64	-3579.31	-3412.43
$\Delta H^\circ_{298}$ (kJ/mol)	-4624.98	-3432.69	-3266.70

ously assigned. The symmetric stretch of the  $\text{ScO}_6$  unit at  $447 \text{ cm}^{-1}$  corresponds very well with the experimental value, as already stated and shows, again, the importance of taking into account the second hydration sphere in the model calculations. The inclusion of the second hydration sphere, denoted  $[\text{Sc}(\text{OH}_2)_6(\text{OH}_2)_{12}]^{3+}$ , or more concisely, [6+12], raises the frequency of the  $\nu_1(\text{ScO}_6)$  mode by  $50 \text{ cm}^{-1}$  (11%), relative to the [6+0] species (cf. the HF/6-31G\* result for Sc[6+0] in Table 7).

The internal modes of the water molecules,  $\nu_2(\text{OHO})$ ,  $\nu_1(\text{H}_2\text{O})$ , and  $\nu_3(\text{H}_2\text{O})$  occur as groups, as inner-sphere and outer-sphere waters. Real electrolyte solutions do not allow such a

convenient differentiation because the water modes are very broad and a differentiation is no longer possible (for electrolyte solution spectra cf., e.g., ref 16 and 20). The coordination of water to a metal ion results in an increase of the frequency of the deformation mode compared to unligated water. The stretching modes on the other hand shift to lower frequencies with coordination of water to a metal ion. This spectroscopic behavior is correctly reproduced by our model.

The SCF binding energy at 0 K for the Sc[6+18] cluster was calculated to  $-4821.64$ ,  $-3579.31$ , and  $-3412.43 \text{ kJ/mol}$  (HF/3-21G, HF/6-31G\*, and HF/6-31+G\*, respectively). The hydration enthalpy for the gas-phase reaction at 298.15 K,  $18\text{H}_2\text{O} +$



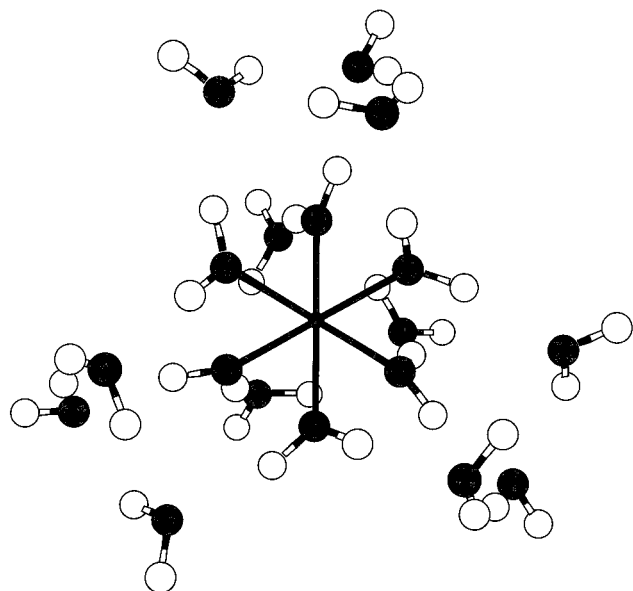


Figure 8. structural model (symmetry  $T$ ) of the  $[\text{Sc}(\text{H}_2\text{O})_{18}]^{3+}$  cluster.

$\text{Sc}^{3+} \rightleftharpoons [\text{Sc}(\text{OH}_2)_{18}]^{3+}$ , follows:  $\Delta H_{298} = \Delta E_{298} - \Delta pV$ , where  $\Delta E_{298} = \Delta E_b^0 + \Delta E_v^0 + \Delta(\Delta E_v)^{298} + \Delta E_r^{298} + \Delta E_t^{298}$ , with the following definitions:  $\Delta E_b$  is the computed difference in the electronic energies of reactants and product at 0 K, including the BSSE correction.  $\Delta E_v^0$  is the difference between the zero-point vibrational energies of reactants and products at 0 K.  $\Delta(\Delta E_v)^{298}$  is the change in the vibrational energy difference between 298.15 and 0 K. (This term arises primarily from thermal population of new low-frequency modes, librations, Sc–O skeletal modes, and intermolecular modes which appear in the cluster as already described).  $\Delta E_r^{298}$  is the change in rotational energies of reactants and product. (Classically, this is equal to  $(-1/2)RT$  for each degree of rotational freedom lost due to cluster formation. So, this term is equal to  $(-51/2)RT$ ).  $\Delta E_t^{298}$  is the translational energy change due to the changes in the number of degrees of translational freedom. (In this reaction, 3 times 18 degrees of freedom are lost, so this term is equal to  $(-54/2)RT$ .) Finally,  $\Delta pV$  is the  $pV$  work term. (Assuming ideal behavior,  $\Delta pV = -18RT$ , since 18 mol of gas are lost in the hydration reaction.)  $\Delta H_{298}$  was calculated to be  $-3432.69$  kJ/mol (HF/6-31G\* level) for the  $\text{Sc}[6+12]$  and is ca. 10% smaller than the single ion hydration enthalpy,  $\Delta H_{\text{hyd}}^0$ , for Sc(III). Two different values for the single ion hydration enthalpy for Sc(III) are reported,  $-3897^{52a}$  and  $-3960$  kJ/mol.<sup>52b,c</sup> The SCF binding energy at 0 K and the gas-phase hydration enthalpy at 298.15 K for the cluster formation are also given in Table 9.

It has to be noted that the experimental and calculated  $\Delta H$  are not strictly comparable, because the experimental value is a hydration enthalpy (aqueous phase) and the calculated value is a binding energy (gas phase). To relate these two values, one would have to include a Born correction and also a correction for the heat of vaporization of water. What the comparison shows here is that these terms roughly cancel, but more accurate calculations would necessitate their inclusion. A similar statement was made for  $\text{Mg}^{2+}$ ,<sup>20b</sup> in which it was shown that one cannot use the bulk-phase water vaporization enthalpy but instead must calculate an explicit 18-water cluster. Because of the lack of symmetry, this would be very difficult. For a given theoretical level, the calculated vaporization enthalpy (binding energy of water clusters) will not converge to the experimental value as the number of waters increases, but to a predicted value for that level. This is not the aim of this study.

TABLE 10: Unscaled HF/6-31G\* Frequencies, Intensities (IR, Raman), and Force Constants of the Octadecaqua Scandium (III) ( $\Gamma_{\text{vib}} = 13a(\text{R}) + 13e(\text{R}) + 40f(\text{IR}, \text{R})$ , and  $\Gamma_{\text{ScO}_6} = a(\text{R}) + e(\text{R}) + 4f(\text{IR}, \text{R})^a$

freq	IR	Raman	f.c.	char.	assignment
30.1	0.088	0.066	0.0025	f	(H <sub>2</sub> O) <sub>3</sub> twist
38.3	0	0.01	0.004	a	(H <sub>2</sub> O) <sub>3</sub> twist
43	0	0.291	0.0057	e	(H <sub>2</sub> O) <sub>3</sub> trans
57.9	2.30	0.0106	0.011	f	(H <sub>2</sub> O) <sub>3</sub> trans
79.3	1.45	0.025	0.0217	f	(H <sub>2</sub> O) <sub>3</sub> trans
108.3	0.002	0.163	0.042	f	translational mode + ScO <sub>6</sub> def.
111.7	15.3	0.129	0.039	f	translational mode + ScO <sub>6</sub> def.
117.0	6.13	0.017	0.0336	f	(H <sub>2</sub> O) <sub>3</sub> H-bond, asym. str.
129.8	1.73	0.0063	0.0413	e	(H <sub>2</sub> O) <sub>3</sub> H-bond, asym. str.
137.8	2.79	0.0148	0.059	f	(H <sub>2</sub> O) <sub>3</sub> H-bond, asym. str.
168.9	7.76	0.08	0.075	f	(H <sub>2</sub> O) <sub>3</sub> H-bond, sym.str.
170.1	0	0.134	0.0756	a	(H <sub>2</sub> O) <sub>3</sub> H-bond, sym. str.
178.6	0	0.044	0.108	a	(H <sub>2</sub> O) <sub>3</sub> H-bond sym. +ScO <sub>6</sub> def
179	0.477	0.0047	0.125	f	ScO <sub>6</sub> def
181.7	0	0.08	0.106	e	(H <sub>2</sub> O) <sub>3</sub> rock
207.2	36.7	0.186	0.175	f	ScO <sub>6</sub> def.
271.1	0.002	0.000	0.196	f	ScO <sub>6</sub> def.
288.7	24.1	0.0046	0.148	f	(H <sub>2</sub> O) <sub>3</sub> rock +ScO <sub>6</sub> def
333.9	45.1	3.23	0.078	f	H <sub>2</sub> O (2) lib.
338.8	0	0.51	0.0776	e	H <sub>2</sub> O (2) lib.
342.4	42.143	0.200	0.082	f	H <sub>2</sub> O (2) lib.
421.3	0.34	3.25	0.426	e	ScO <sub>6</sub> str.
446.7	0	0.37	0.267	a	ScO <sub>6</sub> sym. str.
459.2	0	0.315	0.14	e	H <sub>2</sub> O (2) lib.
474.8	99	4.59	0.147	f	H <sub>2</sub> O (2) lib.
477.4	0	0.53	0.177	a	H <sub>2</sub> O (2) lib. + ScO <sub>6</sub> stretch
482.9	65.3	0.214	0.168	f	H <sub>2</sub> O (2) lib.
493.4	0	1.14	0.161	e	H <sub>2</sub> O (2) lib.
495	195.2	0.26	0.25	f	ScO <sub>6</sub> asym. stretch.
514.4	7.53	0.004	0.21	f	H <sub>2</sub> O (2) lib.
536	150	0.55	0.204	e	H <sub>2</sub> O (2) lib.
540	0	0.54	0.225	e	H <sub>2</sub> O (2) lib.
544.0	0	0.965	0.193	e	H <sub>2</sub> O (2) lib.
549.5	281.8	0.577	0.22	f	H <sub>2</sub> O (2) lib.
649.9	143	2.45	0.189	a	H <sub>2</sub> O (1) wag
670	3.6	0.566	0.275	f	H <sub>2</sub> O (1) twist
719	0	0.09	0.318	e	H <sub>2</sub> O (1) twist
777.5	53	0.09	0.382	f	H <sub>2</sub> O (1) twist
813.3	0	0.7	0.418	a	H <sub>2</sub> O (1) wag
814	419.2	0.065	0.421	f	H <sub>2</sub> O (1) rock
865.5	873	0.7	0.484	f	H <sub>2</sub> O (1) lib.
925.3	154.4	0.166	0.534	f	H <sub>2</sub> O (2) lib
990.3	296.1	0.607	0.618	f	H <sub>2</sub> O (1) rock + H <sub>2</sub> O (1) lib
1818.4	93.1	1.32	2.1035	f	HOH bending outer- sph.
1819	81.7	10.1	2.105	f	HOH bending outer- sph.
1819.1	0	7.5	2.104	f	HOH bending outer- sph.
1823.3	299	1.28	2.117	e	HOH bending outer- sph.
1825.9	0	0.107	2.124	a	HOH bending outer- sph.
1898.1	0	0.754	2.274	e	HOH bending inner- sph.
1904.3	247	0.004	2.288	f	HOH bending inner- sph.
1924.1	0	0.0086	2.325	a	HOH bending inner- sph.
3673.2	0	30.6	8.303	e	OH str. -sym. inner- sph.
3685	930.1	27.5	8.366	f	OH str. -sym. inner- sph.
3712	113.7	8.48	8.848	f	OH str. -sym. inner- sph.
3737.8	3265	123.2	8.966	f	OH str. -sym. inner- sph. + sym. outer- sph.
3751.4	0	472.5	8.683	a	OH str. -sym. inner- sph. + sym. outer- sph.
3978.2	81	11.2	9.788	f	OH str. -sym. inner- sph. + sym. outer- sph.
3978.6	0	510.6	9.791	a	OH str. -sym. inner- sph. + sym. outer- sph.
4005.4	42.4	5.84	9.902	f	OH str. -sym. inner- sph. + sym. outer- sph.
4006	0	33.3	9.90	e	OH str. -sym. inner- sph. + sym. outer- sph.
4006	275.5	3.656	9.901	f	OH str. -sym. inner- sph. + sym. outer- sph.
4103.2	15.2	33.3	10.737	f	OH str. asym. outer- sph.
4105	66.1	5.33	10.733	e	OH str. asym. outer- sph.
4104.8	937.4	0.007	10.743	e	OH str. asym. outer- sph.
4105	0	145	10.75	e	OH str. asym. outer- sph.
4105.5	0	94	10.732	a	OH str. asym. outer- sph.

<sup>a</sup> Harmonic frequencies in  $\text{cm}^{-1}$ ; IR = infrared intensities in  $\text{kmol}^{-1}$ ; Raman scattering activities in  $\text{\AA}^4/\text{au}$ ; force constants in  $\text{mdyne}/\text{\AA}$ .



**3.2.4. NBO Analysis of the Water Clusters.** The NBO (natural bond orbital) method was used to determine the atomic charges. In scandium hexahydrate, the calculations indicate that the charge on Sc is approximately  $2.34e$ , which suggests that  $0.11e$  have been transferred to each water of the first hydration sphere. The oxygens have a charge of  $-1.08e$ , whereas each hydrogen has a charge of  $0.59$ . The polarization, taken as the difference of these two charges, and related to dipole moment, is  $2.26e$ .

In the heptahydrate, the scandium has a charge of  $2.30e$ , and the average water a charge of  $0.10e$ , with the oxygen bearing an average charge of  $-1.06e$  and the hydrogens  $0.58e$ . The waters in the heptahydrate possess a smaller charge and are not as polarized ( $2.22e$ ).

In the octadecahydrate, the scandium has a charge of  $2.28e$ , slightly smaller than in the hexahydrate. The first sphere waters bear a charge of  $0.06e$ , also smaller than the hexahydrate, in which oxygens bear a charge of  $-1.10e$  and hydrogens a charge of  $0.58e$ . The first sphere bears a total charge of  $0.37e$ , much reduced from the  $0.66e$  of the hexahydrate. The remaining charge is taken up by the second sphere waters ( $0.34e$ ). The second sphere thus distributes the charge over the entire complex.

The distribution of the atomic charge as calculated above gives the following. The second sphere waters "allows" the Sc to become slightly less charged ( $0.06e$ ), but more importantly, it draws charge from the first sphere waters ( $0.05e$ /inner sphere water) and shows the long-range delocalization of the charge. The question of polarization of the waters needs to be answered.

The net polarization of the waters does not change by virtue of a change in atomic charge. The net dipole moment of the waters is less because the angle opens and counteracts the increase in length. However, the bond-dipoles of the water would increase along the O–H bond, so in this sense, the water bonds are more polarized. This translates to a greater quadrupole moment of the waters in the first hydration sphere.

#### 4. Conclusions

We showed conclusively that Sc(III) in aqueous perchlorate solution occurs as a hexaaqua complex ion. Ab initio molecular calculations confirm the stability of the hexaaqua ion and that the Sc–O bond length is comparable with the recently found bond length for Sc–O in perchlorate solution by EXAFS. The weak, polarized Raman band assigned to the  $\nu_1(a_{1g})$   $\text{ScO}_6$  mode of the hexaaqua Sc(III) ion ( $T_h$  symmetry for the whole complex ion or  $O_h$  symmetry for the  $\text{ScO}_6$  unit) has been studied. The isotropic scattering geometry in R format was employed in order to measure the true vibrational contribution of the band and account for the Boltzmann temperature factor  $B$ . The dependence on concentration has also been measured. The  $442\text{ cm}^{-1}$  band of hexaaqua Sc(III) shifts only  $3\text{ cm}^{-1}$  to lower frequencies and broadens about  $20\text{ cm}^{-1}$  for a  $60^\circ\text{C}$  temperature increase. The Raman spectroscopic data suggest that the hexaaqua Sc(III) ion is stable in perchlorate solution over the temperature range measured. These findings are in contrast to  $\text{ScCl}_3^-$  solutions where chloride replaces water of the first hydration sphere.

Besides the polarized component at  $442\text{ cm}^{-1}$ , two weak depolarized modes at  $295$  and  $410\text{ cm}^{-1}$  were measured in the Raman effect. These two modes of the  $\text{ScO}_6$  unit of the hexaaqua ion were assigned to  $\nu_2(e_g)$  and  $\nu_5(f_{2g})$ , respectively. The infrared active mode  $\nu_3(f_{1u})$  was measured to be at  $460\text{ cm}^{-1}$  (taken from Adams, D. M. *Metal–Ligand vibrations and related vibrations*; E. Arnold: London, 1967).

Ab initio geometry optimizations of  $[\text{Sc}(\text{OH}_2)_6]^{3+}$  were carried out at the Hartree–Fock and second-order Møller–

Plesset levels of theory, using various basis sets up to  $6\text{-}31\text{+G}^*$ . The vibrational frequencies of the  $[\text{Sc}(\text{OH})_6]^{3+}$  cation were also calculated. The theoretical binding energy for the hexaaqua Sc(III) ion was calculated and accounts for ca.  $54\text{--}60\%$  of the experimental hydration enthalpy of Sc(III).

The stability of the hexaaqua scandium(III) cluster could be demonstrated by comparing the stability of the  $[\text{Sc}(\text{OH}_2)_6(\text{OH}_2)]^{3+}$  cluster with the  $[\text{Sc}(\text{OH}_2)_7]^{3+}$  cluster, resulting in the stability of the former.

The frequency calculations and the thermodynamic parameters for the  $\text{Sc}[6+12]$  cluster are given, and the importance of the second hydration sphere is stressed.

**Acknowledgment.** The assistance of a scholarship (PGSB, PDF) granted by NSERC to C.C.P. is gratefully acknowledged. The authors thank the Computing and Communications Department, Memorial University of Newfoundland, for computer time, with a special thanks to DEC for providing an Alpha server 4100. W.W.R. thanks Dr. M. H. Brooker for the use of his Raman spectrometer and his hospitality during the stay at MUN/Nfld. W.W.R. also states that the results quoted in ref 35 were unfortunately only published in E. German local papers. W.W.R. thanks Prof. S. Schönherr, the former group leader at the Mining Academy Freiberg, Department of Chemistry, for his support.

**Supporting Information Available:** Tables S1–S9 showing optimized geometries of  $[\text{Sc}(\text{OH}_2)_n]^{3+}$  ( $n = 1\text{--}9$ ) and Table S10 showing BSSE and deformation corrections of  $\text{Sc}[6+1]$  and  $\text{Sc}[7+0]$  (energies are given in kJ/mol). This material is available free of charge via the Internet at <http://pubs.acs.org>.

#### References and Notes

- (1) Burgess, J. *Metal Ions in Solution*; E. Horwood: Chichester, 1978; pp 137–159.
- (2) Marcus, Y. *Chem. Rev.* **1988**, *88*, 1475–1498.
- (3) (a) Kanno, H.; Yamaguchi, T.; Ohtaki, H. *J. Phys. Chem.* **1989**, *93*, 1695–1697. (b) Kanno, H.; Yoshimura, Y. *J. Alloys Compd.* **1995**, *225*, 253–256.
- (4) Yamaguchi, Y.; Niihara, M.; Takamuku, T.; Wakita, H.; Kanno, H. *Chem. Phys. Lett.* **1997**, *274*, 485–490.
- (5) *Gmelins Handbuch der anorganischen Chemie, Scandium* (System Nr. 39); Verlag Chemie: Weinheim/Bergstrasse, 1973; Part A2, p 47 and references therein. The following crystallographic values of the ionic radius were given. The ionic radius of Sc(III) was mostly recognized for compounds with oxygen, and a value of  $0.83$  and  $0.68\text{ \AA}$  was given in the older literature, for example: Strunz, H.; Tennyson, C. *Mineralogische Tabellen*, 5th ed.; Leipzig, 1970; p 331, 387. Newer results on synthetic compounds show, that a smaller ionic radius of  $0.73\text{ \AA}$  has to be taken. Compare, for example: Fondel, C. Z. *Kristallogr.* **1968**, *127*, 121–138. On the other hand, in the well-known inorganic text by Cotton and Wilkinson (Cotton, F. A.; Wilkinson, G. *Advanced Inorganic Chemistry*, 5th ed.; Wiley: New York, 1988; p 973) a value of  $0.68\text{ \AA}$  is given for the ionic radius for Sc(III).
- (6) Valkonen, J. *Ann. Acad. Sci. Fenn., Ser. A2* **1979**, *188*, 36.
- (7) Casterliani, C. B.; Carugo, O.; Giusti, M.; Sardone, N. *Eur. J. Solid State Inorg. Chem.* **1995**, *32*, 1089–1099.
- (8) Fratiello, A.; Lee, R. E.; Schuster, R. E. *Inorg. Chem.* **1970**, *9*, 391–392.
- (9) Rudolph, W. W.; Brooker, M. H.; Pye, C. C. *J. Phys. Chem.* **1995**, *99*, 3793–3797.
- (10) Moskovits, M. *Proceedings of the Fifth International Conference on Raman Spectroscopy*; Freiburg, Germany, 2–8 September, 1976; p 768–769. Michaelian, K. H.; Moskovits, M. *Nature* **1978**, *273*, 135–136.
- (11) Nash, C. P.; Donnelly, T. C.; Rock, P. A. *J. Sol. Chem.* **1977**, *6*, 663–670.
- (12) Bulmer, J. T.; Irish, D. E.; Oedberg, L. *Can. J. Chem.* **1975**, *53*, 3806–3811.
- (13) Irish, D. E.; Jarv, T. *Chem. Soc. Faraday Discuss.* **1978**, *64*, 95 and 120.
- (14) Rull, F.; Balarev, Ch.; Alvarez, J. L.; Sobron, F.; Rodriguez, A. J. *Raman Spectrosc.* **1994**, *25*, 933–941.
- (15) Walrafen, G. E. *J. Chem. Phys.* **1962**, *36*, 1035–1042; **1966**, *44*, 1546–1558.

- (16) (a) Rudolph, W. Z. *Phys. Chem.*, **1996**, *194*, 73–95. (b) Rudolph, W. W.; Brooker, M. H.; Tremaine, P. R. *Z. Phys. Chem.* **1999**, *209*, 181–207.
- (17) Brooker, M. H.; Fauriskov Nielsen, O.; Praestgaard, E. *J. Raman Spectrosc.* **1988**, *19*, 71–78.
- (18) Högfeldt, E. *Stability Constants of Metal-Ion Complexes*; Pergamon Press: Oxford, 1982; , Part A, p 204.
- (19) (a) Pye, C. C.; Rudolph, W.; Poirier, R. A. *J. Phys. Chem.* **1996**, *100*, 601–605. (b) Pye, C. C. *Int. J. Quantum Chem.* **2000**, *76*, 62–76.
- (20) (a) Rudolph, W. W.; Pye, C. C. *J. Phys. Chem. B* **1998**, *102*, 3564–3573. (b) Pye, C. C.; Rudolph, W. W. *J. Phys. Chem. A* **1998**, *102*, 9933–9943. (c) Rudolph, W. W.; Pye, C. C. *Phys. Chem. Chem. Phys.*, **1999**, *1*, 4583–4593.
- (21) Vogel, A. I.; *A Text-Book of Quantitative Inorganic Analysis*, 3rd ed.; Longman: London, 1961; p 415.
- (22) Harris, W. E.; Kratochvil, B. *An Introduction to Chemical Analysis*; Saunders College Publishing: Philadelphia, 1981; p 75 and 203.
- (23) Brown, P. L.; Ellis, J. Sylva, R. N. *J. Chem. Soc., Dalton Trans.* **1983**, 35–36.
- (24) Cole, D. L.; Rich, L. D.; Owen, J. D.; Eyring, E. M. *Inorg. Chem.* **1969**, *8*, 682–685.
- (25) (a) Hehre, W. J.; Stewart, R. F.; Pople, J. A. *J. Chem. Phys.* **1969**, *51*, 2657–2664. (b) Pietro, W. J.; Hehre, W. J.; *J. Comput. Chem.* **1983**, *4*, 241–251.
- (26) (a) Binkley, J. S.; Pople, J. A.; Hehre, W. J. *J. Am. Chem. Soc.* **1980**, *102*, 939–947. (b) Dobbs, K. D.; Hehre, W. J. *J. Comput. Chem.* **1987**, *8*, 880–893.
- (27) (a) Hehre, W. J.; Ditchfield, R.; Pople, J. A. *J. Chem. Phys.* **1972**, *56*, 2257–2261. (b) Hariharan, P. C.; Pople, J. A.; *Theor. Chim. Acta (Berlin)* **1973**, *28*, 213–222.
- (28) Huzinaga, S. *Gaussian Basis Sets for Molecular Calculations*; Elsevier: Amsterdam, 1985.
- (29) Frisch, M. J.; Trucks, G. W.; Schlegel, H. B.; Gill, P. M. W.; Johnson, B. G.; Wong, M. W.; Foresman, J. B.; Robb, M. A.; Head-Gordon, M.; Replogle, E. S.; Gomperts, R.; Andres, J. L.; Raghavachari, K.; Binkley, J. S.; Gonzalez, C.; Martin, R. L.; Fox, D. J.; Defrees, D. J.; Baker, J.; Stewart, J. J. P.; Pople, J. A. *Gaussian 92/DFT*, revision F.4; Gaussian, Inc.: Pittsburgh, PA, 1993.
- (30) Glendening, E. D.; Reed, A. E.; Carpenter, J. E.; Weinhold, F. *NBO*, version 3.1.
- (31) Rudolph, W. W.; Pye, C. C. *Z. Phys. Chem.* **1999**, *209*, 243–258.
- (32) Adams, D. M. *Metal-Ligand vibrations and related vibrations*; E. Arnold: London, 1967.
- (33) (a) Rudolph, W. Diploma Thesis, Mining Academy Freiberg, Department of Inorganic and Inorganic-Technical Chemistry, Freiberg/Saxony, 1979. (b) Rudolph, W.; Schönherr, S. *Z. Phys. Chem. (Leipzig)* **1989**, *270*, 1121–1134. (c) Rudolph, W.; Schönherr, S. *Z. Phys. Chem. (München)* **1991**, *172*, 31–48. (d) Rudolph, W.; Schönherr, S. *Z. Phys. Chem. (München)* **1991**, *173*, 167–177.
- (34) *Gmelins Handbuch der anorganischen Chemie, Seltenerdelemente, Teil C5, Sc, Y, La, und Lanthanide (System Nr. 39)*; Verlag Chemie: Weinheim/Bergstrasse, 1977; pp 235–238 and references therein.
- (35) Rudolph, W.; Schönherr, S. *Proceedings of the Chemical Society of the GDR, Halle (Saale)*; 2–4 December, 1986; p 83. To produce the Al(III), Ga(III), and In(III) chloride and perchlorate solutions, the metals were dissolved in concentrated HCl and HClO<sub>4</sub>, respectively (with a few drops of mercury salt in order to speed up reaction). The perchlorate spectra of Ga(III) and In(III) gave two polarized modes which were not consistent with octahedral hexaaqua ions. As it turned out, ClO<sub>4</sub><sup>−</sup> was reduced by the metals to Cl<sup>−</sup>, which then, like chloride salts, formed chloro complexes of the general nature [Ga(OH)<sub>2</sub>6−*n*Cl<sub>*n*</sub>]<sup>+(3−*n*)</sup> and [In(OH)<sub>2</sub>6−*n*Cl<sub>*n*</sub>]<sup>+(3−*n*)</sup>, respectively. A more recent Raman study on aqueous solutions of Al(III), Ga(III), and In(III) in both the liquid and glassy state is given by (a) Kanno, H.; Hiraishi, J. *Mem. Defense Acad. Jpn.* **1987**, *11*–27. (b) Kanno, H.; Hiraishi, J. *J. Chem. Phys. Lett.* **1979**, *68*, 46–48.
- (36) Paul, A. D. *J. Phys. Chem.* **1962**, *66*, 1248–1252.
- (37) Reed, G. L.; Sutton, K. J. Morris, D. F. C. *J. Inorg. Nucl. Chem.* **1964**, *26*, 1227–1231.
- (38) Samodelov, A. P. *Radiokhimia* **1964**, *6*, 568–581.
- (39) Kraus, K. A.; Nelson, F.; Smith, G. W. *J. Phys. Chem.* **1954**, *58*, 11–17.
- (40) Šmirous, F.; Celeda, J. Palek, M.; *Collect. Czech. Chem. Commun.* **1971**, *36*, 3891–3899.
- (41) (a) Rudolph, W. W.; Irmer, G. *J. Solution Chem.* **1994**, *23*, 663–684. (b) Rudolph, W. W.; Brooker, M. H.; Tremaine, P. R. *J. Solution Chem.* **1997**, *26*, 757–777. (c) Rudolph, W. W. *Ber. Bunsen-Ges. Phys. Chem.* **1998**, *102*, 183–196. (d) Rudolph, W. W. *J. Chem. Soc., Faraday Trans.* **1998**, *92*, 489–500.
- (42) Diaz-Moreno, S.; Muñoz-Páez, A.; Martínez, J. M.; Pappalardo, R. R.; Marcos, E. S. *J. Am. Chem. Soc.* **1996**, *118*, 12654–12664.
- (43) Rudolph, W. W. *Z. Phys. Chem.* **2000**, *215*, in press.
- (44) Åkesson, R.; Pettersson, L. G.; Sandström, M.; Wahlgren, U. *J. Am. Chem. Soc.* **1994**, *116*, 8691–8704; **1994**, *116*, 8704–8713.
- (45) Rotzinger, F. P. *J. Am. Chem. Soc.* **1997**, *119*, 5230–5238.
- (46) Glendening, E. D.; Feller, D. *J. Phys. Chem.*, **1996**, *100*, 4790–4797.
- (47) Hartmann, M.; Clark, T.; van Eldik, R. *J. Am. Chem. Soc.* **1997**, *119*, 7843–7850.
- (48) Rudolph, W. W.; Pye, C. C. Memorial University of Newfoundland, Department of Chemistry, 1995, unpublished material. Pye, C. C. Ph.D. Thesis, Memorial University of Newfoundland, Department of Chemistry, 1997.
- (49) Even the strongest bonds include more or less anharmonic contributions. The dilemma is that for the weak ScO<sub>6</sub> mode no such data are available, whilst for monomeric water, the anharmonicity corrections are well-known. Therefore, the ab initio frequencies, which can at best reproduce harmonic frequencies, may be compared directly to (harmonic) experimental frequencies. From literature compilations, it can be deduced that the harmonic frequency of  $\nu_1(\text{ScO}_6)$  should be ca. 10 cm<sup>−1</sup> higher than the measured one (Jones, L. H. *Inorganic Vibrational Spectroscopy*; Marcel Dekker: New York, 1971; Vol. 1, Chapter 1). The anharmonicity cannot be the deeper reason for the above-described deviation.
- (50) Muñoz-Páez, A.; Pappalardo, R. R.; Marcos, E. S. *J. Am. Chem. Soc.* **1995**, *117*, 11710–11720. Muñoz-Páez, A.; Diaz, S. Perez, P. J. Martin-Zamora, M. E.; Martínez, J. M.; Pappalardo, R. R.; Marcos, E. S. *Physica B* **1995**, *208/209*, 395–397.
- (51) Pavlov, M.; Siegbahn, P. E. M.; Sandström, M. *J. Phys. Chem. A* **1998**, *102*, 219–228.
- (52) (a) Smith, D. W. *J. Chem. Educ.* **1977**, *54*, 540. (b) Burgess, J. *Ions in Solution*; Ellis Horwood Publishers: Chichester, 1988; Chapter 4, Table 4.7. (c) Richens, D. T. *The Chemistry of Aqua Ions*; John Wiley: Chichester, 1997; Appendix.